FLOODING DAMAGE DETECTION FROM POST-HURRICANE SATELLITE IMAGES

B. Tech. Project Stage-II Report

Submitted by

Akanksha Thorat	**111803108**
Amey Dhongade	**111803110**
Divya Alone	**111803114**

Under the guidance of

Mr. Suraj T. Sawant

College of Engineering, Pune

DEPARTMENT OF COMPUTER ENGINEERING AND INFORMATION TECHNOLOGY,

COLLEGE OF ENGINEERING, PUNE-5

April-May 2022

DEPARTMENT OF COMPUTER ENGINEERING AND INFORMATION TECHNOLOGY, COLLEGE OF ENGINEERING, PUNE

CERTIFICATE

Certified that this project, titled ""FLOODING DAMAGE DETECTION FROM POST-HURRICANE SATELLITE IMAGES" " has been successfully completed by

Akanksha Thorat	**111803108**
Amey Dhongade	**111803110**
Divya Alone	**111803114**

and is approved for the partial fulfilment of the requirements for the degree of "B. Tech. Computer Engineering".

SIGNATURE

Mr. Suraj T. Sawant

Project Guide

Department of Computer Engineering and Information Technology, College of Engineering Pune, Shivajinagar, Pune - 5.

SIGNATURE

Dr. Vahida Z. Attar

Head

Department of Computer Engineering and Information Technology, College of Engineering Pune, Shivajinagar, Pune - 5.

report-4

ORIGINALITY REPORT

12/04/2022

14%	8%	12%	0%
SIMILARITY INDEX	INTERNET SOURCES	PUBLICATIONS	STUDENT PAPERS

PRIMARY SOURCES

1	arxiv.org Internet Source	1%
2	kilthub.cmu.edu Internet Source	1%
3	Molan Zhang, ZhiQiang Chen. "Deep Metric Learning for Damage Detection Using Bitemporal Satellite Images", 2021 IEEE International Geoscience and Remote Sensing Symposium IGARSS, 2021 Publication	1%
4	Xiaohua Tong, Zhonghua Hong, Shijie Liu, Xue Zhang, Huan Xie, Zhengyuan Li, Sonlin Yang, Weian Wang, Feng Bao. "Building-damage detection using pre- and post-seismic high-resolution satellite stereo imagery: A case study of the May 2008 Wenchuan earthquake", ISPRS Journal of Photogrammetry and Remote Sensing, 2012 Publication	1%
5	Takashi Miyamoto, Yudai Yamamoto. "Using Multimodal Learning Model for Earthquake	1%

Abstract

Damage assessment is one of the most efficient approaches to attain this goal. Disaster experts have recently employed satellite pictures or drone images to determine flood damage in urban areas. Convolutional Neural Networks (CNN) will be utilised in this study to detect the damage caused by floods. To train the model, we will use a dataset posted by NOAA during Hurricane Harvey. Using this dataset we aim to find damages done particularly to buildings and roads. We will use 12 CNN models:- VGG-16, Resnet50,Inception-v3, Alexnet, Densenet, Shufflenet, Squeezenet, Googlenet, Wideresnet, Resnext,Mobilenet-v3 and a custom convolutional architecture.

Contents

Chapter 1

Introduction

When a hurricane hits the coast, emergency managers must assess the situation and damage caused by the flood to effectively respond to the disaster and allocate resources for future rescue and recovery work. The traditional practice of assessing disaster and damage conditions relies heavily on several emergency response teams and volunteers that tour the affected area and conduct assessments. However, this process is labor-intensive and time-consuming.[1] Thanks to the advancement in computer vision studies, scientists have found another way to improve the effectiveness of damage assessments. Specifically, we will be applying an image classification algorithm to distinguish damaged buildings and floodplains from undamaged buildings. Moreover, damages done to roads will be detected, so an escape route can be developed by the first responders.

1.1 Importance of Damage Detection

One of these disasters, Hurricane Sandy, resulted in a significant increase in losses and damage. Hurricanes are deadly, wreaking havoc on human life and property. Hurricanes are extremely powerful storms. A hurricane causes incalculable loss of life and property.[2]

In recent times, satellite photography has become increasingly popular for monitoring disaster damage. By giving overhead views, satellite images aid in the assessment of the situation. However, because this procedure is still controlled by humans, it is time-consuming and unreliable. This is where computer vision enters the picture.

1.2 Our Aim

We aim to assess and detect damages done to buildings and roads due to hurricanes by studying the post-event satellite images using CNN. For this purpose we will be using 12 models using CNN architechture that is Resnet VGG,Inception-v3, Alexnet, Densenet, Googlenet, Shufflenet, Squeezenet,Wide resnet, Resnext, Mobilenet-v3 and a custom model.These models were chosen because they are better at dealing with vanishing gradient problems, and networks with many layers can be trained without significantly increasing the training error, and they can categorise a wide variety of images with a efficient feature representation. In the identification and better classification of structure damage detection due to floods. Using data optimization and data augmentation techniques, we seek to improve the overall accuracy which will helpful in taking preventive measures before the calamities(floods) cause damage.

1.3 Previous Work

Before the CNN era, methods for assessing flood risk were established, including precipitation analysis, catchment capacity, river network analysis, flood contour and depth generation based on topology data, and flood spread simulation. There were also probabilistic risk assessments or definitions of infrastructure system vulnerability indicators. These methods are still valuable today, as natural disasters are natural phenomena that follow physical rules. However, these observations provided the hypothesis that there may be potential improvements in the post-hurricane damage assessment process when using multiple data types.Remote sensing based on machine learning approaches, where photos is being researched to lessen damage and vulnerability to environmental damages such as the quake Ranjbar 2018 and the avalanche Ada 2018. Hong2018, Tsunami Mehrotra2015, Wildfire Lu2018.[3] While such a method is very promising, it takes advantage of the unique characteristics of each hazard and cannot be applied directly to damage assessment in post-hurricane images.

1.4 Use of Deep Learning and Geo-spatial Images for Detecting Damage

The impact a natural calamity can cause is very calmitous and becomes very difficult while assessing. Moreover, the nearby residents lives are also at a risk. Object-based image damage-detection using pre- and post-earthquake photos, as well as deep learning models and architectures, will aid in the understanding of the situation.

1.5 Next Sections

In the next sections, we have included literature review conducted on building and road damage detection, the research gaps observed from the literature review, the objective of our project, methodologies proposed, dataset chosen and a preferred timeline.

Chapter 2

Literature Review

[1] **Cao, Q. & Choe, Y., 2021.** - Building damage annotation on post-hurricane satellite imagery based on convolutional neural networks.

[2] **Kaur, S., Gupta, S., Singh, S., Koundal, D. & Zaguia, A., 2021.** - Convolutional Neural Network based Hurricane Damage Detection using Satellite Images. [online] Available at: https://assets.researchsquare.com/files/rs-934531/v1/61a71f08-c163-442b-a62e-1af4cdc8708d.pdf?c=1632928070.

[3] **Cao, Q. & Choe, Y., 2021.** - Post-Hurricane Damage Assessment Using Satellite Imagery and Geolocation Features. [online] Arxiv.org. Available at: ¡https://arxiv.org/pdf/2012.08624.pdf¿ [Accessed 20 November 2021].

[4] **Masanobu Shinozuka, Roger Ghanem, Bijan Houshmand, Babak Mansouri (2000)** - The paper follows SAR Simulation Methodology and conducts rapid assessment of the location and extent of urban seismic damage by identifying damage signatures in SAR images. The accuracy of the derived DEM is limited by factors such as system noise and multiple reflections of radar signal. The dataset used by this paper was NASA's CV990 airborne L-band SAR images. Since this approach takes only SAR images, it is expected to yeild a lower accuracy.

[5] **Gilles Andre, Lucian Chiroiu, Catherine Mering, Franck Chopin (2003)** - The paper follows morphological anomalies research method. The method seems to offer new possibility and opportunity for the detection of severe damages after an earthquake. The limitation of this paper is that some kinds of strong damages to buildings (that collapse on its base without tilt) stay undetectable. Less than 1% of buildings considered as damaged are unaffected buildings. The dataset used by this paper was Ikonos Images.

Using this method, there is a very small chance that a building detected as damaged could be undamaged.

[6] **Marco Chini, Christian Bignami, William J. Emery, Nazzareno Pierdicca, Salvatore Stramondo (2003)** - The paper follows morphological features extraction method from pre-event and post-event images. The approach classifies buildings into one of three possible damage level: Light or No-Damage, Medium and Heavy. Although, the comparison between the results and a damage map from ground survey has not been conducted extensively. 55% of buildings were detected as heavily damaged in the heavily damaged area found using ground survey 38% were detected at lightly damaged in lightly affected areas. The dataset used was Quickbird. This method's results aren't very accurate, but the results are encouraging.

[7] **K. Kouchi, F. Yamazaki (2004)** - The paper follows Visual interpretation, Pixel-based and Object-based detection approach. A comparison between all approaches was carried using their user and producers accuracies.The determination of appropriate indices like edge and shape information needs to be worked on for better accuracy. User's Accuracy of pixel-based was higher - 23.2% and producer's accuracy of object-based approach was higher - 49.98%. The dataset used was Quickbird.

[8] **Fumio Yamazaki, Ken'ichi Kouchi, Masayuki Kohiyama, Nanae Muraoka, Masashi Matsuoka (2004)** - The paper has followed Visual Interpretation method. Using the post-event pan-sharpened images, buildings surrounded by debris, partially collapsed buildings and totally collapsed buildings were identified by 5 interpreters. It was difficult to reach a consensus for identifications of "moderate damage" or "partially collapsed" cases. The dataset used was Quickbird. This method relies upon individual perspective and hence is non-reliable.

[9] **F. Yamazaki, Y. Yano, M. Matsuoka (2005)** - The paper follows Visual interpretation and Automated damage detection. Post-event IKONOS and Quickbird images were employed in an automated damage detection method. The resultant damaged areas agreed reasonably well with the visual inspection results and the field survey data. Some amount of omission error was observed due to the limitation of near-vertical images with 0.6m resolution. The method gave an accuracy rate of 88%. Combining results from two datasets improved the overall accuracy.

[10] **S. Stramondo, C. Bignami, N. Pierdicca, M. Chini (2007)** - The paper has demonstrated the possibility to significantly improve the results taking advantage of the change detection potential of the InSAR complex coherence combined with optical data. A decrease of accuracy was observed due to: the lower resolution of ASTER data and the higher spatial baseline of the interferometric SAR pairs. Accuracies found for Bam case-study - 77% and Izmit case-study - 90%. The datasets used were Optical IRS, SAR from ER-1 and ER-2, Optical TERRA-ASTER, SAR ENVISAT-ASAR images.

[11] **Mustafa Turker, Emre Sumer (2008)** - Watershed Segmentation of the post-event aerial pictures is used in the paper. The approach has a precision of 80.63 %. GCM, Turkey Images, was the data set used. The article only considered buildings that are rectangular in shape, making it impossible to quantify the impact of other shaped structures.

[12] **M. Kawamura, K. Tsujino, T. Shimada, Y. Tsujiko (2010)** - The research is about the weighted-cost distance function was used to obtain a broad picture of the damage and emergency route situation while using the suggested GIS to determine an emergency transportation route. The detection accuracy was at 66-68 %, and the analyses' dependability was found to be around 26 %. The dataset utilised was SPOT's NDVI. Due to the identification of miss-detection pixels, the findings for flat and hilly areas are not accurate enough.

[13] **ZHANG Yong, JIANG Yulin, XU Jian, WU Zhongyi, HONG Zixuan, LIU Xianglong, (2010)** - The strategy and architecture for assessing highway disasters using GIS and RS are described in this study. The research provides two methods for detecting highway disasters. The paper's limitation is that there were radiation inaccuracies due to atmospheric scattering and absorption, as well as lighting conditions. The accuracy discovered was 70-75 %. FORMOSAT2 was the dataset used. To swiftly create the slope map and aspect map, they used ArcScene from ArcGIS desktop.

[14] **Chandana Dinesh Parape, Masayuki Tamura (2011)** - The method used in this paper is Differential Morphological Profiling. Using connected components analysis on pixels picked based on their morphological features, the building footprint was retrieved in a region. Overfitting of the decision surface to the data could result in error extraction of building structure. The ISODATA training gave confidence metrics that

suggested the post-event dependability was 88.46%. IKONOS PAN photos were utilised as the dataset.

[15] **Shunichi Koshimura, Shintaro Kayaba and Hideomi Gokon (2011)** - The paper uses spectral radiation properties to undertake image analysis. Tsunami numerical models are used to assess damage in the paper. Instead of clubbing, the study separates the area segment into multiple different classes and determines the damages to each particular class, resulting in no overall results. The user satisfaction levels range from 57% to 97%. Quickbird was the dataset used. Definiens Professional was utilised in the paper for segmentation and object-oriented classification.

[16] **Zhonghua Hong, Shijie Liu, Xue Zhang, Huan Xie, Zhengyuan Li, Sonlin Yang, Weian Wang, Xiaohua Tong, Feng Bao (2012)** - Two methods for detecting collapsed buildings were proposed: one was to compare the height differences of building corner points to detect an individual collapsed building, and the other was to calculate the difference between the pre- and post-seismic DEMs generated from pre- and post-seismic stereo images to detect the region of collapsed buildings. The discovered accuracy was 94 % -95%. The data set used was IKONOS. From the before and after damage images, with the aid of three dimensional positions,with the aid of the corner point of the buildings and difference of their height improved results wwere obtained.

[17] **Pralhad Upret and Fumio Yamazak (2012)** - This article looked at radar features like the correlation coefficient and the backscattering difference between two SAR images collected at different periods. Pre- and post-event analysis results were proven to be useful in detecting building damage in low, moderate, and high density locations. When fusing satellite SAR photos, a low detection ratio for the high-density area was discovered. Overall, 73.8 % of the time was correct. TerraSAR-X was the dataset used. In places with a high density of buildings, the strategy is ineffective.

[18] **Laigen Dong, Jie Shan (2013)** - Multi-temporal strategies that analyse changes between pre- and post-event data, as well as mono-temporal procedures that only interpret post-event data, were used in this study. An in-depth assessment of a large number of building damage detection systems indicated that they were designed in accordance with the unique characteristics of the applied data and the affected area in almost every case. Although a quantitative comparison evaluation of all of these approaches is impossible because none of them can be verified using one or more sets of experimental data.

Overall, 71.4 percent of the people were successful. The datasets used were Quickbird, Worldview, and IKONOS. The technique was tested on three different datasets: SAR, optical, and LiDAR images.

[19] **Haijian Ma, Nan Lu, Linlin Ge, Qiang Li, Xinzhao Yu, Xiaoxuan Li (2013)** - The research recovers road damage from remote sensing photographs, as well as road features and changes after earthquakes, using edge and line detection. Road maps are used not only to offer pre-earthquake road information, but also to aid in the extraction of road segments from post-earthquake pictures, and it depends on geometric aspects rather than spectral properties. It was discovered that the accuracy was 86%. The dataset utilised was Quickbird.

[20] **Mona Peyk herfeh, Asadollah Shahbahrami, Farshad Parhizkar Miandehi (2013)** - The Adaboost and Neural Network techniques are used in this paper.Because of its simplicity, a weak classifier (CART) was utilised. The accuracy rate was 84%. Quickbird was the dataset used. The report stated that neural networks require substantially less time to implement and are also easier to use.

[21] **Hideomi Gokon, Masashi Matsuoka, Erick Mas, Shunichi Koshimura, Wen Liu, Bruno Adriano (2013)** -The study employs indices to detect the spread of the impacted area, as well as a phase-based change detection method that employs NDVI and NDWI. POC analysis gives accurate data for emergency response following natural disasters. Typhoons can modify the ground cover across large distances, making it more difficult to retrieve damaged areas. The accuracy was determined to be 73%. ASTER VNIR was the dataset used. In this work, three bands on VNIR images are employed, and the thresholds for various amounts of damage have been carefully chosen.

[22] **Yongxin CAO , Yan CHEN, Ling TONG, Youchun LU,Xirui ZHANG, Mingquan JIA (2013)** - Utilized the Duda operator for finding the possible structures and eliminate other information which dramatically reduces the impact noise has on the detection. The accuracy was determined to be 76%. RadarSat-2 was the dataset used. By selecting a better segmentation threshold, you can improve accuracy.

[23] **Reza Hassanzadeh, Zorica Nedovic-Budic (2014)** - The study covers satellite imagery data and picture analysis, pixel-based analysis, visual analysis, and crowdsourced analysis. The average accuracy levels increased when the results of predictive

modelling and RS data were merged, demonstrating that employing CS as a direct value boosted average accuracy levels. Because of the limited direct association between CS and AE data based on the coincidence of buildings included in both datasets, the average accuracy fell across all pairs of data sources evaluated. The average accuracy rate was found to be 48.5 percent. The dataset utilised was Quickbird. The essay compares crowd-sourced data with three different damage detection algorithms.

[24] **Qiming Qin ,Jianhua Wang, Jianghua Zhao , Xin Ye , Xuebin Qin, Xiucheng Yang , Jun Wang , Xiaopo Zheng , Yuejun Sun (2015)** - In the research discussed, it talks on the understaning of the relation of the destroyed road strcutres as well as the analysis from the images of the roads after the disaster. The use of the center of the road to replace the data before the damage occured is novel in this approach, as it removes the impact of missing pre-disaster data. The road boundary is blurred by mixed pixels, which reduces the accuracy of damage identification. The accuracy gained was 90%. Worldview-1 was the data set used. Better enhancing algorithms, which can enhance accuracy despite mixed pixels with road and other land markers, are among the improvements.

[25] **Moslem Ouled Sghaier, Richard Lepage (2015)** - On the road surface and the retrieved objects, multiscale segmentation for the transfroms on the wavelet is conducted. Finally, the Dempster Shafer theory evaluates which item mapping to a membership section. Shadow images aren't taken into account. The KNN model performs better than the dst model. Haiti tpr is 78 percent and bourmedes -91 percent. Geoeyes was the data set used. SSD could help with improvements such as precision.

[26] **Milad Janalipour and Ali Mohammadzadeh (2015)** - The research uses decision to decide the adapting infrastructure fuzzy logic system (ANFIS) model that efficiently recognised building damage degree using geometric aspects of post-event buildings. TO make better building damage identification using spatial-textural features. is another upcoming project. The accuracy rate was 80%. Quickbird was the data set that was used. SVM, textural characteristics, and correlation coefficients could be used to increase accuracy. The creation of a fuzzy inference system.

[27] **Lionel Gueguen Raffay Hamid (2015)** - In terms of precision, B-LLC has a equivalence of B-SIFT, although it is less efficient. Finally, compared to CNNs, the

recommended utilisation SD characteristics requires 13 times less time. The damage-detection framework will be used to a broader class of changes in the future, such as recognising urbanisation patterns and harbour and border surveillance. The Guided Model has a true positive rate of 74%, while the Exhaustive Model has a tpr of 88%. DigitalGlobe was employed as a data source. To improve accuracy, more subset clustering techniques are being used.

[28] **David Dubois (2015)** -Using optical pictures gathered before and after the event decision making system, the paper uses an array classification method to get a better building damage evaluation. In comparison to unsupervised correlation methods, a guided damage assessment classification can produce better results. With fewer training data, it's possible that processing time will increase without a significant improvement in accuracy. PAP1, PAP2, BOU1, and BOU2 had mean accuracies of 84.5 percent, 70.4 percent, 71.7 percent, and 54.5 percent, respectively, for the various datasets. The Guided Model is accurate. Quickbird was the data set that was used. Accuracy can be improved by combining SDD or SVM with random forest algorithms.

[29] **Edward T.-H, Chu Chung-Chih Wu (2015)** - To estimate seismic damage inside buildings, the article uses IDEAS, an image-based disaster impact management system. Even if there are large number of video cameras installed, it rapidly and automatically analyses the damage once an earthquake occurs. Accuracy rate was 97.6%. Hurricanes, floods, and typhoons are all expected to cause harm in the future.

[30] **Aydan Menderes a , Arzu Erener , Gülcan Sarp (2015)** - The paper discerns beofre and the after image change with the help Of dsm methology of using patches. nDSM was subjected to a change analysis. A changed view angle or optical system could make it difficult for the change analysis to identify the collapsed buildings. Overall accuracy was 96.54 percent for Region-1, Region-2 90.74 percent. Use of random forest method with lidar photos is something that will be explored in the future.

[31] **Fatih Kahraman , Mumin Imamoglu , Hasan F. Ates (2015)** - The paper uses a similarity classifier to detect changes in buildings, that has been seen to be resistant to changes in lighting and tiny local deformations. Building footprints are useful mitigating false positives caused by changes in non-building areas. Building patches and building footprints focusses on structural damages of each specific building thinking alot on the surrounding environment. Better building design could improve the SSD model.

The true positive rate is 72 percent, whereas the false positive rate is 29 percent. Support vector machines, as well as the SSD model, will be added in the future.

[32] **Jihui Tu , Wenqing Feng ,Zhina Song, Haigang Sui(2016)** -The paper uses data from models of 3D Geographic information system and remote sensing pictures where images after the structure damage for remote sensing using the 3 dimensional geoinformatic model system or remote procedure call parameters initially are corrected. 91.25% is the accuracy.To improve accuracy, future study will include the utilisation of oblique aerial photos and public source images.

[33] **Wen Liu , Rendy Bahri, Tadashi Sasagawa ,Fumio Yamazaki(2016)** - According to the paper, the Corelation Coefficient was estimated using TerraSAR-X images, which provide preliminary proof of the havoc to built environments. The data set used was TerraSAR-X, which had an accuracy of 84.2 percent (TSX). The utilisation of sar and lidar imagery, as well as svm, will be used in future studies to detect damage to the six key buildings.

[34] **Chao Wang , Lixia Gong ,Jingfa Zhang , Hong Zhang , Fan Wu, Qiang Li (2016)** - The paper utilizes a specific post-earthquake inter range VHR SAR picture and original structure layout data to assess damage to buildings. The method can be used to assess whether a building is demolished or still standing after an earthquake, and it avoids the problems of locating accurate edges for identifying building damage. 89.1% is the accuracy. TerraSAR-X was the data set used. For higher accuracy, future study will include employing k nearest neighbours.

[35] **Mumin Imamoglu ,Fatih Kahraman Hasan F. Ates (2016)** - Utilized detailed model which characterises structure neighbourhoods improves detection accuracy.The algorithm computes similarity factor. For damaged structures, the MRF technique yields tpr of 85/83 percent and fpr 20/18 percent mapping to subset-1 and subset-2, respectively. UNOSAT was the data set used.

[36] **D.M. Hordiiuk V.V. Hnatushenko (2016)** - The map of the smooth surface is achieved by utilizing the Laplace filter locally in the paper. The gradient values and the Laplacian second-order values are used to establish a result for every picture pixel. The accuracy rate is 78 percent. Images of Long Island were utilised as the data set.

Future study will greatly aid in calculating damage implications and give more precise measures than are now available.

[37] **Young-Jin Cha , Wooram Choi ,Oral Buy uk ozt urk(2017)** - The research then goes on to show how CNNs may be used to create a predictor for identifying cement fractures in photos. The initial goal is to create a classifier model that is less affected by disturbance induced by illumination, shadow projection, and blur, as well as to provide a broad range of flexibility. Furthermore, feature extraction approaches are unnecessary since CNN learns features automatically when the network is modified using Stoichastic gradient descent. When compared to I.P.T, this benefit can save a lot of time and work. In training and validation, the accuracy was 98.22% out of 32K photos and 97.95% out of 8K images, respectively.

[38] **Ken Sakurada†,Ryosuke Nakamura, Tomoyuki Imaizumi,Riho Ito,Aito Fujita, Shuhei Hikosaka,(2017)** - The article then goes on to classify whether or not a structure has been corroded away by water. Data contains beofre and after images that surround the intented building in the centre. The accuracy ranges from 94 to 96 percent. The ABCD dataset was used. Future research will look into CNNs that can recognise and identify entities from beginning to end.

[39] **Ram C. Sharma , Ryutaro Tateishi, Keitarou Hara, Hoan Thanh Nguyen, Saeid Gharechelou , Luong Viet Nguyen (2017)** - The report uses the EDV framework to visualise earthquake-induced building damage. The accuracy rate was 86% SAR pictures from JAXA dataset. To offer new perspectives on emergency planning, such as changing construction codes in sensitive fracture zones.

[40] **Zixiang Zhou, Jie Gong (2018)** - In aerial LiDAR data, the paper uses a complex neural network classifier and identify residential construction objects.It does not require any well before geometric or textural properties. Automatically check building items from point cloud data with various densities and structure situations (damaged, intact, or collapsed) using a CNN-based technique.With good mapping functions. Recall:0.895 and Precision:0.865. The LIDAR dataset was used. Future research will look into various surface architectures inside the artificial learning network to increase building detection accuracy even more.

[41] **Jigar Doshi Saikat Basu Guan Pang (2018)** -The research offers a model called DII which uses the analysis from the detection with the CNN, which can then

be thresholded and clustered together. The Disaster Impact Index DII is created by clustering and thresholding the change masks obtained from CNN outputs. It can be used to identify priority zones for relief efforts. Hurricane Harvey flooded the area. Accuracy: Precision: 88.8 recall: 50.5 for DII-based road change prediction vs. marked effect area. FRAP impact area precision:81.1 % recall:73.5 % DII-based building change prediction vs. FRAP impact area precision:81.1 percent Spacenet spa (2018) and Deepglobe Demir et al. data sets were used (2018). Future study will include using knn or svm to calculate the impact of disasters on other natural and man-made features.

[42] **Hiroya Maeda, Yoshihide Sekimoto, Toshikazu Seto, Takehiro Kashiyama and Hiroshi Omata (2018)** -The accuracy and runtime performance of the damage detection model were tested on both a GPU server and a smartphone. Finally, it was demonstrated where the destruction caused can be broken into 8 classes of remarkable identification. While using MobileNet and Inception V2, we were able to achieve recall and precision rates of around 71% and 77%, respectively. In the future, increase the amount of training data and create the structure of a new neural network to improve the detection accuracy of difficult-to-detect categories. A pixel-by-pixel technique could be used to detect road degradation.

[43] **Qiang Li, Lixia Gong, Jingfa Zhang (2018)** -Based on textural aspects of pre- and post-earthquake SAR images, the article uses a watershed segmentation-based object-level damage building identification approach. The approach used the watershed segmentation algorithm to partition the PCs of texture characteristics after obtaining the optimal texture features. Overall, there is an accuracy rate of 89.3 %. The data collection used was photographs from the Advanced Land Observing Satellite-1 (ALOS-1). Future research will incorporate polarisation features to further improve detection accuracy.

[44] **Konstantin Pogorelov, Michael Riegler, Olga Ostroukhova, Pål Halvorsen, Kashif Ahmad,Nicola Conci, Rozenn Dahyot (2019)** - The subject of flood classification and flood aftermath detection using social media and satellite data is addressed in this research. To determine if a vehicle will be able to pass the road, Convolutional Neural Networks and a transfer learning-based categorization approach are utilised. The proposed methods are tested on large-scale datasets such as ImageNet & Places. The accuracy of this model was around 62.3 %, and it may have been higher if the CNN-GAN approach had been utilised in conjunction with a larger dataset.

[45] **Wenhan Lu, Zebo Li,Joseph Z.Xu,Pranav Khaitan, Valeriya Zaytseva (2019)** -This study compares the performance of four different convolutional neural network models in detecting damaged structures. They created custom data sets for three disasters: Haiti's 2010 earthquake, Mexico City's 2017 earthquake, and Indonesia's 2018 earthquake.Their methods help in better aliging of photos for better results.

[46] **Niloofar Khodaverdi Zahraee, Heidar Rastiveis, Arash Jouybari (2019)** - An object-based approach combining LiDAR raster data and high-resolution satellite imagery (HRSI) was developed to assist the relief operation by recognising building damage. A Worldview II satellite image and LiDAR data of Port-au-Prince, Haiti, captured after the 2010 earthquake were used to test this method. The categorization was classified into three groups based on the object-level analysis: "Undamaged," "Probably Damaged," and "Certainly Damaged," with an overall accuracy of 92 %.

[47] **Edward J. Hoppe, Fabrizio Novali, Alessio Rucci, Alfio Fumagalli, Sara Del Conte,Giacomo Falorni,Nora Toro (2019)** - The findings of two post tensioned bridges in Virginia are monitored and presented in this research. On an 11-day interval, the TerraSAR-X radar satellite was utilised to capture radar pictures in the Staring SpotLight mode. The data was analysed using the SqueeSAR algorithm, which gave the time-displacement series millimeter-range precision.

[48] **Diogo Duarte, Fabio Giulio,Francesco Nex Tonolo, Norman Kerle (2019)** -This work employs an enhanced CNN with dense connections and dilated convolutions. Satellite, airborne, and UAV photos collected from Geo-Eye1 and Worldview-3, encompassing numerous locations: L'Aquila (Italy), Port-au-Prince (Haiti), Portoviejo (Ecuador), Amatrice (Italy), Pesc. Tronto (Italy), Kathmandu (Nepal), Sukabumi (Indonesia), Sukabumi (Indonesia), Su (Indonesia). The categorization produces image patches that indicate whether the image is damaged or undamaged. The model's accuracy ranged from 87.1% to 93.9 % . When low-resolution data and datasets with varying quality and spatial resolutions were employed, poor results for new sites were seen.

[49] **S. Ghaffarian, N. Kerle (2019)** - This work offers a CNN-based approach to detect damages from remote sensing pictures, and structural rubble/debris has been implemented to better detect damage detection. Both UAV, multi-temporal satellite photos with a spatial resolution of 0.5 are analysed. GeoEye1, WorldView2 and WorldView3

photos, as well as Pleiades, were used to create the images. For higher accuracy, they recommend using daily data for this model.

[50] **Irwan Meilano, Achmad Ikbal Rahadian, Deni Suwardhi, Wulan Suminar, Fiza Wira Atmaja, Cecep Pratama, Euis Sunarti, Setya Haksama (2020)** -This research examines building damage caused by tsunamis, with Palu's 2018 example serving as the case study. Object recognition utilising pre-trained YOLOv3 models from high-resolution satellite imagery data was used to create the location and number of buildings. Object detection was carried out before and after the tsunami, with an accuracy of 76.78 % and 74.20%, respectively, for building distribution data. The findings revealed that there was a strong link between building damage and wave height.

[51] **Feihong Zhao ,Jingyuan Bao, Delie Ming (2020)** - This research proposes a strong multi-feature technique for recognising damaged structures using satellite pictures and building footprints before and after an event. The MRF (Markov Random Field) context model is also used. There is no published dataset of war-affected places to use as a benchmark in the literature. As a result, Google Photographs' 2017 satellite images of Ar Raqqa, Syrian Arab Republic, were picked, which included extremely high quality optical satellite images with a spatial resolution of 0.6m. The overall accuracy of the model is up to 83 %.

[52] **You He, Gang Li ,Yu Liu, Xiao Jiang, Xiao-Ping Zhang (2020)** -A new superpixel-based belief fusion (SBBF) model for detecting building deterioration is presented in this research. To execute superpixel-level fusion on the SAR and optical pictures, segmentation on the pre-earthquake optical image is used to identify the superpixels. Then, to increase the accuracy of building damage detection, an unique belief fusion method that uses a basic belief assignment (BBA) to accommodate diverse reliabilities of superpixels is developed. In this experiment, three datasets were used: Quickbird and COSMO-Skymed (coastal area of Port-au-Prince), Quickbird and COSMO-Skymed (city), GeoEYE-1 and RADARSAT-2, with accuracy of 99.18 %, 98.10 %, and 98.55 %, respectively.

[53] **Sang-Eun Park,Sun-Gu Lee (2020)** - This research provides a new urban change detection approach that comprises morphological operations for extracting building areas and morphological indices for detecting damage-related changes. Kompsat-5 SAR photos were employed, which provide a long temporal baseline and a variety of

observational situations. On December 20, 2015 (pre-event) and October 24, 2017 (post-event), two enhanced standard mode data from the Kumamoto region were collected for this study (post-event). According to the findings, combining a morphological building index with unique scattering processes in urban areas reduced false alarms in natural changes and enhanced detectability in building-damaged areas.

[54] **Ritwik Gupta, Nirav Patel, Richard Hosfelt, Sandra Sajeev, Matthew Gaston, Eric Heim, Jigar Doshi, Bryce Goodman,Keane Lucas, Howie Choset (2020)** - This is a draught report for xBD, a novel large-scale dataset for humanitarian and disaster recovery research to improve change detection and building damage assessment. For pre- and post-event multi-band satellite imagery from a variety of disaster occurrences, xBD provides building polygons, category labels for damage categories, ordinal labels of damage level, and matching satellite metadata. The collection includes bounding boxes and names for environmental factors such as fire, water, and smoke.

[55] **Lucia Saganeiti, Federico Amato, Gabriele Nolè, Marco Vona, Beniamino Murgante (2020)** - The research offers a novel approach integrating Interferometric analysis and the Phase to Displacement algorithm, which is based on the utilisation of SAR and LiDAR data to quickly assess seismic damage in the early post-event phases. In August 2016, the concept was applied to a case study of the municipality of Amatrice (Central Italy). The orthophotos from 1988, 1998, and 2006, as well as DigitalGlobe, were used to create this model. The classification's overall accuracy is 63 %. They argue that proper application of this approach necessitates greater access to this data.

[56] **Rohit Gupta, Mubarak Shah (2020)** - The RescueNet model proposed in this paper is a unified model that can segment buildings and assess damage levels to individual buildings while being trained end-to-end with a novel localization aware loss function that consists of a Binary Cross Entropy loss for building segmentation and a foreground only selective Categorical Cross-Entropy loss for damage classification. The method was tested on the xBD dataset and yielded an overall accuracy of 73.4 percent. By creating improved methodologies for resolving discrete building instances, they intend to improve both building localization and damage assessment in the future.

[57] **Takashi Miyamoto, Yudai Yamamoto (2020)** - There are two steps to the scheme suggested in this paper. First, they use information from a GIS database about the placements and shapes of the buildings to determine the photographic scope of each

house in wide-area photographic photos and extract small photographic fragments at the level of individual structures. Second, they use a dataset collected from satellite images of the afflicted area in the 2016 Kumamoto Earthquake in Japan to assess the damage to residential structures in the impacted area, using a classifier to determine whether these individual fragments indicate collapsed structures. The total accuracy of the model is 73.5 /

[58] **Quoc Dung Cao, Youngjun Choe (2020)** -The research proposes using image classification algorithms on post-hurricane satellite photos to better detection of structures. 'Flooded/Damaged' or 'Undamaged' are the two output categories. A convolutional neural network is built from the ground up, trained, then compared to a widely used neural network for common object classification. This model's overall accuracy is said to be 97 %..

[59] **Wenjun Zhang , Li Shen, Wenfan Qiao (2021)**- The research provides a system for recognising damaged structures from pre- and post-disaster VHR satellite pictures that combines multi-scale segmentation and scene change detection (MSSCD). In the aftermath of the 2010 Haiti earthquake, they compared the efficiency of four alternative scene categorization frameworks in detecting damaged buildings. The model's accuracy is roughly 96.15 %.

[60] **Molan Zhang, ZhiQiang Chen (2021)** - This paper proposes a novel deep metric learning technique for multi-hazard damage detection in remote-sensing (RS) images. The model is constructed using a triplet network, which addresses the challenge of accurately detecting disaster-induced damage in built-objects utilising pre- and post-event RS data. This is the dataset that the xBD dataset was based on. The average accuracy rate is more than 89 %, and the recall and f1 scores are also satisfactory. The current approach, according to the article, requires pre- and post-disaster photos, which limits its applicability when pre-event images are unavailable.

Chapter 3

Current Research Gaps

1. Overfitting problem in building detection, thereby misclassifying damaged structures as not damaged.Shadows in the images may cause a missclassification thereby reducing the accuracy.

2. Noisy datasets contain images in which structures arent very clear, potentially leading to a mixed pixel problem. Moreover, due to atmospheric scattering, can lead to noisy data, due to which the number of pre-event images avaiable are less, which can affect training the mdoel.

3. Unable to detect the internal features of the structures for early action.Due to calamities such as typhoons, getting information on land cover extraction for datasets becomes very diffcult.

Chapter 4

Objectives

1. Correctly detecting damaged structures using CNN architechture(Resnet-50, VGG-16, Inceptionv3, Alexnet, Densenet). The models can be trained with many images without a significant training error.

2. Improving the accuracy by removing minimizing the problems caused by overfitting by using regularisation, data augmentation and optimization techniques.

3. Improving the classification by creating better clusters for damaged and non damaged structures.To be able to classify as damaged and not damaged irrespective of the view or angle of the image.

4. To correctly detect images even with mixed pixels thereby improving the accuracy.By improving segmentation in the classification for better detection.

Chapter 5

Problem Statement

Developing a damage detection system based on Convolution Neural Network to make it easy for rescuers and first responders to assess damage done to buildings and areas due to flooding. The project will make use of post-hurricane satellite images.

Chapter 6

Methodology

6.1 Pre-Trained Models

6.1.1 Model Architecture

In this project, we have used VGG 16,Resnet 50, Alexnet, Densenet, Inceptionv3, Shufflenet, Squeezenet, Wideresnet, Resnext, Mobilenet-v3, Googlenet models as our 5 pre-trained models and we have also implemented a custom model

VGG-16

The models are deep learning image classifiers that are at the forefrontof technological innovation. VGG 16 employs 33 convolutional layers piled on top of each other to increase depth and 2 X 2 max pooling layers to reduce volume. [64] VGG16 is used in many deep learning image classification problems. However it also has a downside that it is very slow to train and uses significantly more memory than other architectures.

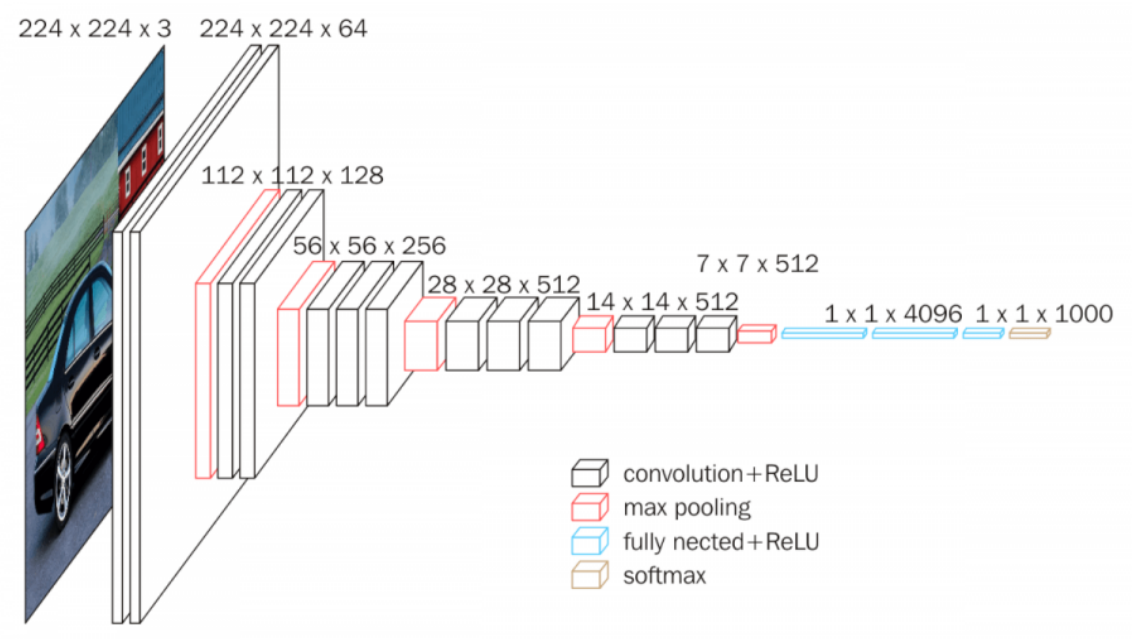

Figure 6.1: VGG-16 Implementation

Resnet50

Resnet50 is comparable to VGG-16, except it has the capacity to map identities. The input size is 224 x 224 x 3, which is processed using a four-stage design. [65] It may stack more layers to create a deeper network, and it also makes use of the Identity Connection, which protects the network from vanishing gradient issues by enabling it to skip past levels that aren't as important in training. [65] Resnet50 is substantially quicker than VGG16 at training and allows for much larger networks.

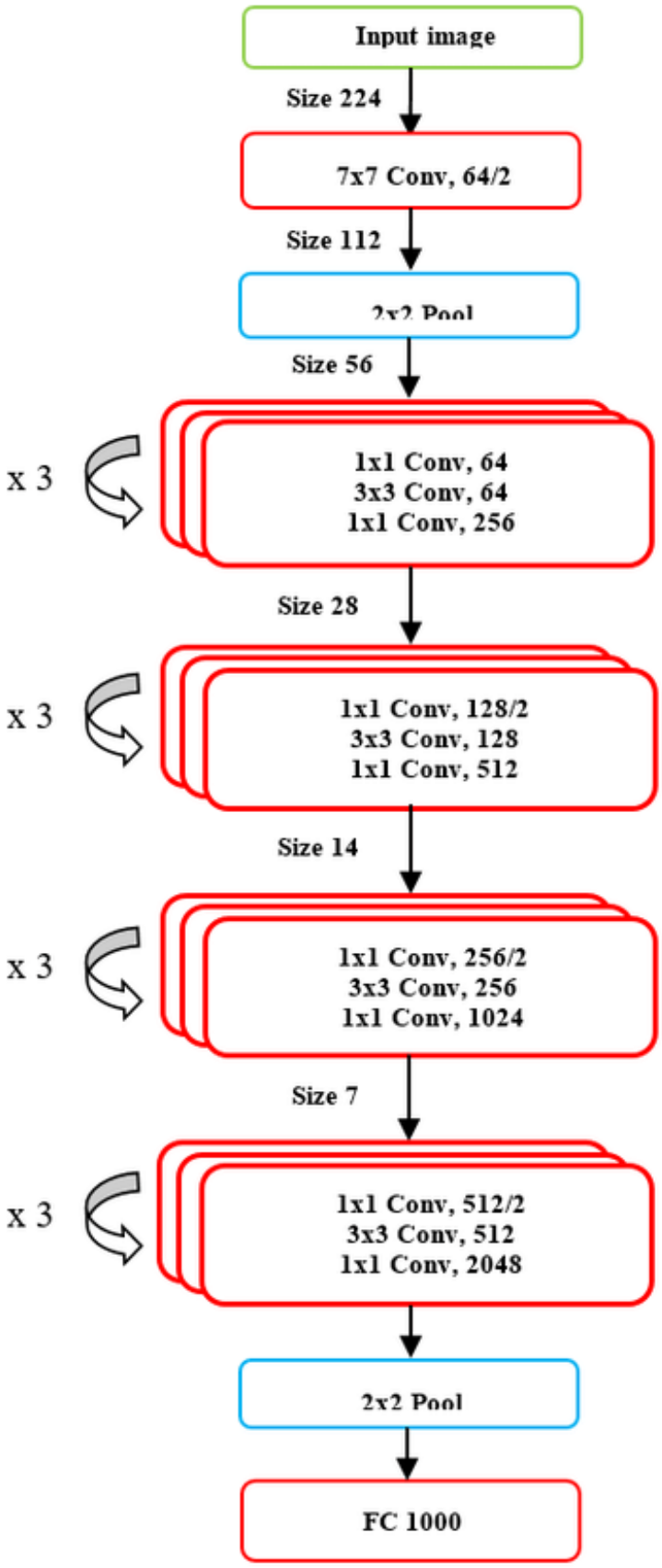

Figure 6.2: Resnet50 with 4 stage architecture

Alexnet

AlexNet contains 8 levels. For the first two convolutional layers, an Overlapping Max Pooling layer is applied after each convolutional layer. Levels in third, fourth, and fifth layers are all linked together. After the fifth convolutional layer comes the Overlapping level, which is containing overlapped layers completely. The use of Max Pooling can help to reduce overfitting. It essentially uses a max operation to pool groups of features, resulting in a smaller number of them. The sole difference between Max Pooling and Overlapping is that the adjacent windows where the maximum is computed overlap.

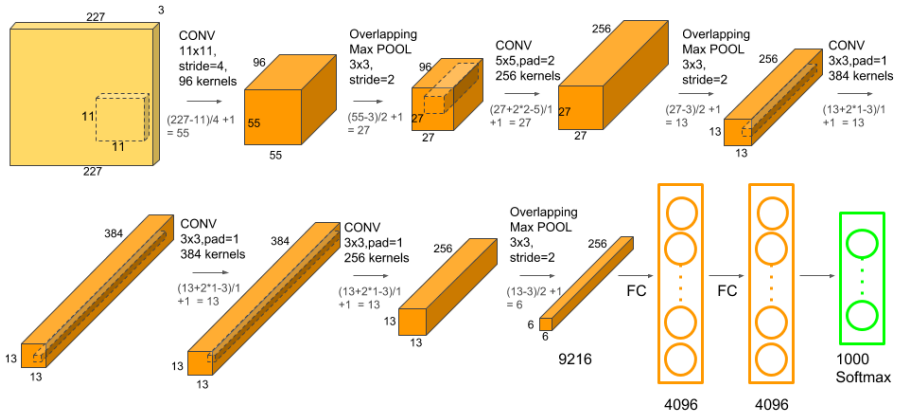

Figure 6.3: Alexnet

Densenet

In the model, all the layers are interconnected. The formula for the number of connections is n(n+1)/2, given that there are n layers. Aside from the fundamental convolutional and pooling layers, DenseNet has two crucial pieces. Dense Blocks and Transition Layers are the two types of Dense Blocks. In densenet, each layer of the densenet network is accompanied by a transition level and then again accompanied by a densenet dense block level. In the end of the densenet structure, there is a classification level.

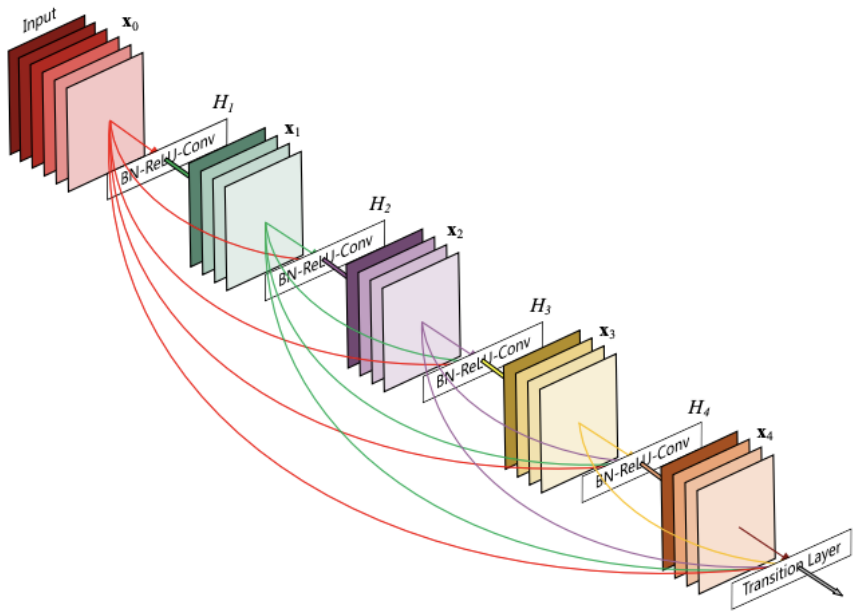

Figure 6.4: Densenet

Inception V3

Inception-v3 is a 42-layer CNN architecture from the Inception family that improves on previous versions. For improved model adaption, the model employs a number of strategies for improving the network.

Batch normalisation is done to activation inputs and is utilised extensively throughout the model. Softmax is used to calculate loss.

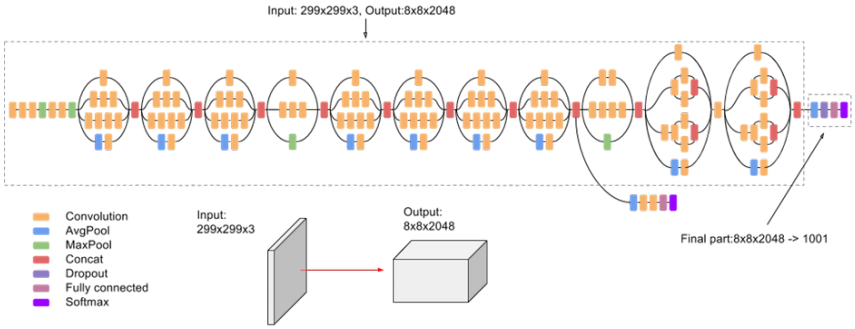

Figure 6.5: Inception V3

Squeezenet

SqueezeNet is a cnn of 18 levels, which is trained using the Imagenet databse. This method returns a SqueezeNet v1.1 network, which has the same accuracy as SqueezeNet

v1.0 but utilises less floating-point operations per prediction.

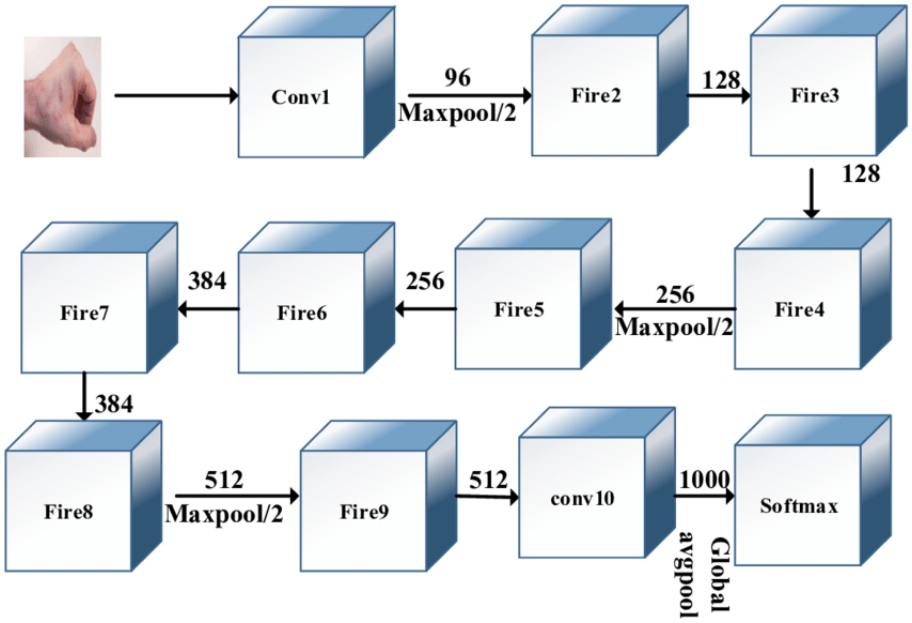

Figure 6.6: Squeezenet

Mobilenet-v3

MobileNets are using in deep cnn for the creation of the levels.We provide in-depth analysis of resource and accuracy tradeoffs, as well as promising ImageNet classification results when compared to other popular models. MobileNets' performance is then proved across a wide range of applications and use cases, including object recognition, fine-grain classification, facial features, and large-scale geolocation.

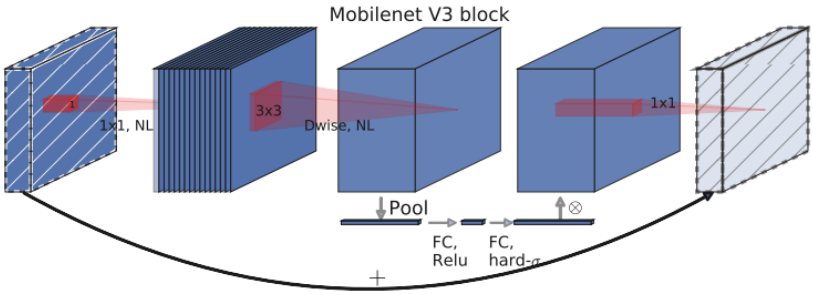

Figure 4. MobileNetV2 + Squeeze-and-Excite [20]. In contrast with [20] we apply the squeeze and excite in the residual layer. We use different nonlinearity depending on the layer, see section 5.2 for details.

Figure 6.7: Mobilenet-v3

WideResnet

The network can be shallower with the same or higher accuracy by widening the Residual Network (ResNet). With a shallower network, the number of layers can be lowered, as well as the training time. Many factors are examined in WRNs, including the ResNet block design. It is k times broader than ResNet when k 1.

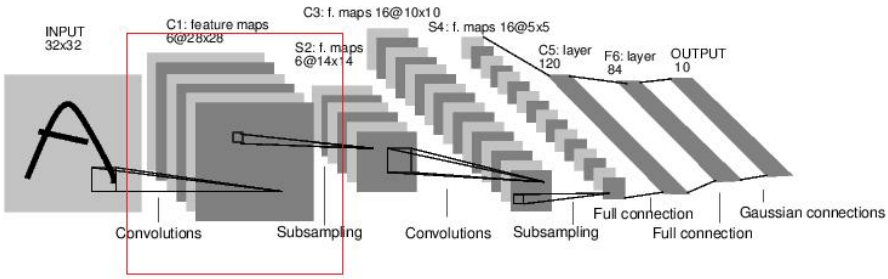

Figure 6.8: WIderesnet

First, a convolution layer of 3x3 size with output of 32x32. A second convolution layer is used with 3x3 size and output of 32x32. Third convolution layers of same size is used with output of 16x16 size. The fourth layer has a output size of 8x8. After that an avg pool layer(8x8) is used for 1x1 output size.

Resnext

A ResNeXt is a structure that combines a group of transformations with the same topology. In comparison to a ResNet, it adds a third dimension to the depth and breadth dimensions: cardinality (the size of the collection of transformations).

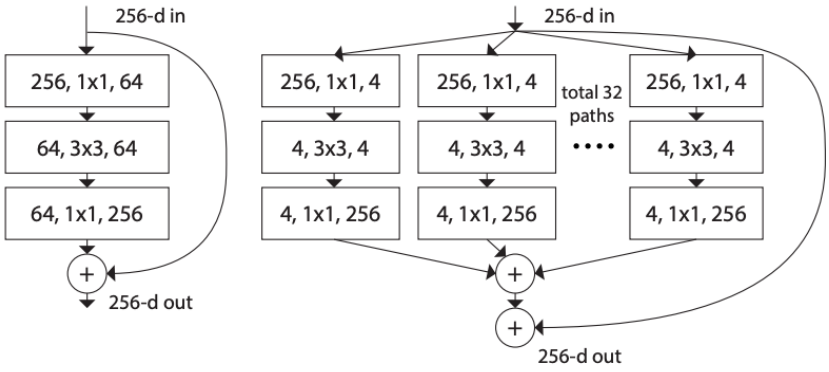

Figure 6.9: Resnext

Shufflenet

The proposed network is mostly made up of a three-stage stack of ShuffleNet units. On the number of channels, a scale factor s is applied. There are certain version of presented such as Shufflenet - 1 and s, meaning that number of the fileters implemented in the netwrok is increased by a factor of s.

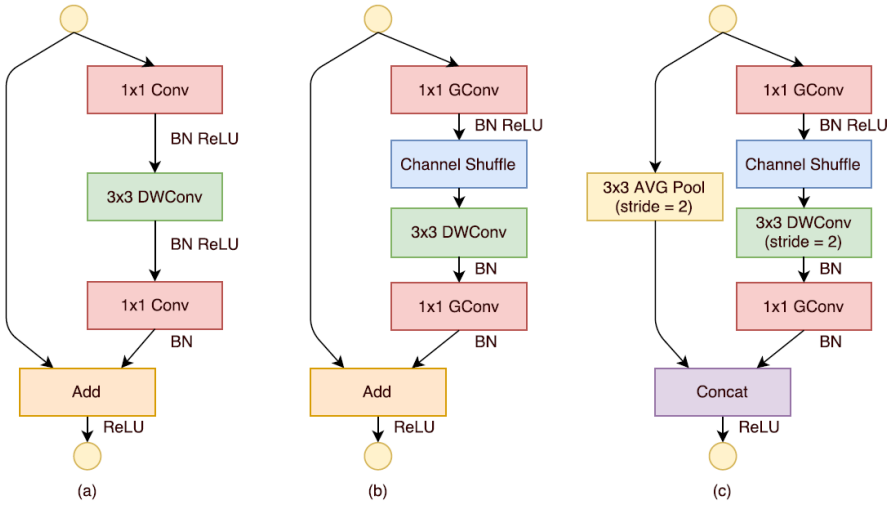

Figure 6.10: Shufflenet

Googlenet

Filters of various sizes can function on the same level in the GoogleNet architecture. Rather than becoming deeper, the network expands. The GoogleNet Architecture has a total of 22 layers, including 27 pooling layers. There are a total of 9 inception modules layered in a linear fashion.

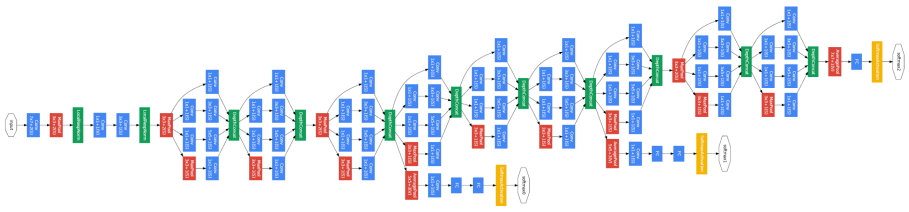

Figure 6.11: Googlenet

6.1.2 Custom Model

In this section we will look into the custom model we will be proposing which will help overcome some of the research gaps. Model Architecture The custom model will be built as a network that contains 8 layers with weights. It follows the block design pattern,

where convolutional layers, 2 fully connected layers, and three pooling (subsampling) layers are layered as a single learning block as seen in figure. The whole model will be formed by the learning layers, the ReLU Activation Layer and the other one is Batch Normalization Layer.

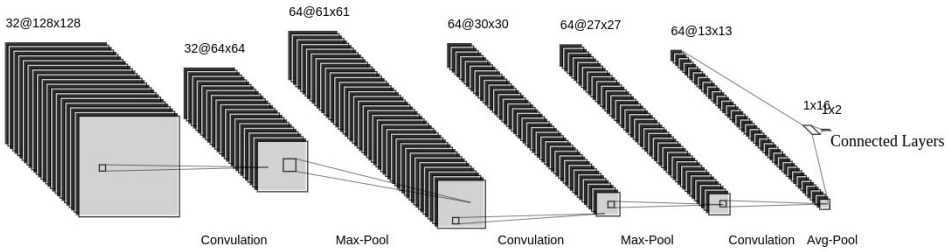

Figure 6.12: LeNet Style Diagram of the 8 layer Custom Network

6.1.3 Implementation

The first part of the experiment is to implement with pre-trained architectures. First step is to load the data we are using followed by setting up the models. After setting the models up, there are some changes that need to be done in order to custom the architecture in order to make it useful according to our aim.

Image Augmentation: These pretrained architectures, like the rest, require the height and width of an input image to have at least 224 pixels, hence we resize the image size from 128 X 128 to 224 X 224.

Connected Layer: In order to modify it for our own use, we will first freeze the existing lower CNN levels, and substitute the complete overlap layersc with a custom classifier, where the amount of output variables is equivalent of the classifications made (2 classes) in the dataset.

Criterion:CrossEntropyLoss function is implemented. [63]

After the changes, the model is evaluated and prediction takes place to find the Accuracy and Confusion Matrix for each pre-trained model

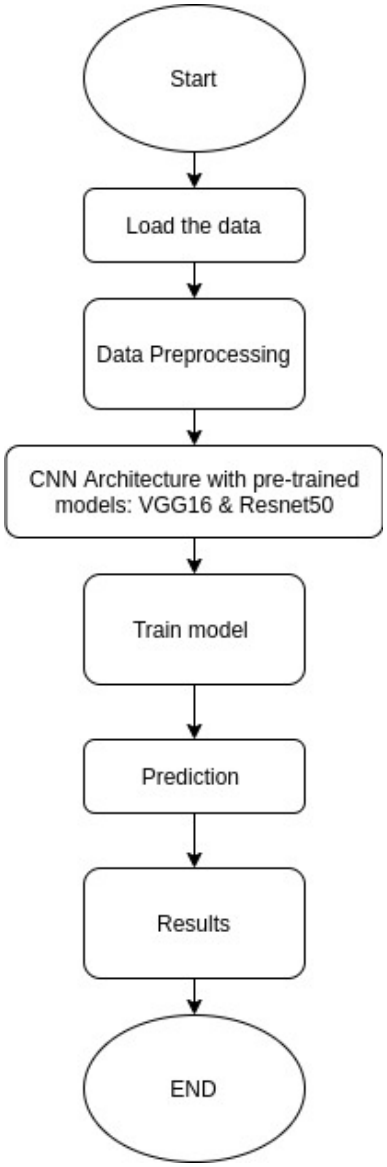

Figure 6.13: Pre-Trained Model Flow Diagram

6.2 Custom Model

6.2.1 Model Architecture

The custom model will be constructed as an 8-layer network with weighted layers. As shown in Figure, 3 convolutional layers, 2 fully connected layers, and three pooling (sub-sampling) layers are layered as a single learning block.Three learning blocks will make up the entire model, which will be supplemented by two completely connected layers. The ReLU Activation Layer is among the convolution layers, and the Batch Normalization Layer is the other.

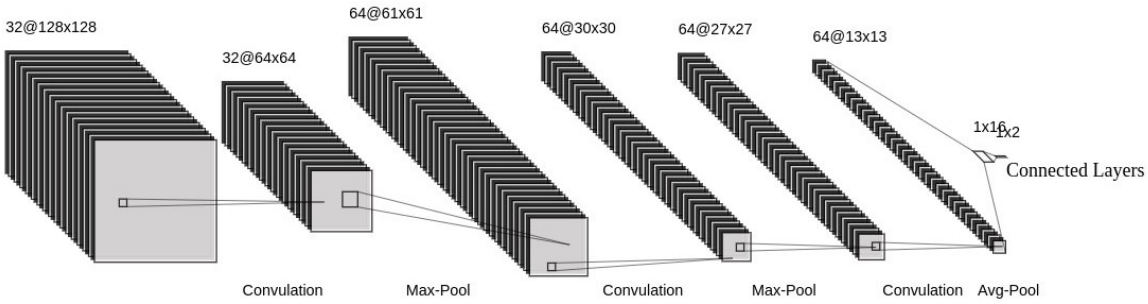

Figure 6.14: LeNet Style Diagram of the 8 layer Custom Network

6.2.2 Implementation

The first steps of implementing the model on the dataset is loading the data and training it. After setting up the trained data, the CNN model is implemented. The custom model having 8 layers is used. The network is divided in 3 phases: Input layer, Feature extraction and Classification. The Extracting Features phase includes three convolutional layers and three pooling layers. Each calculation results in a feature map being extracted as from input data. [61] Pooling layers consist of 2 major layers which are Max-Pool layer and Avg-Pool layer. Levels of max-pool are placed among convolution network.Its objective emphaizes on lowering of dimensionality of an input representation, which lessens overfitting. It takes maximum of the area from the data that the kernel has covered. [61] The Avg-Pool Layer is like the Max-Pool Layer, only it takes the region's average.

In the next phase of Classification , we have the two fully connected layers : Relu,batch Norm function.Relu gives the model nonlinear behavior, allowing it to learn complicated transformations between input data and target variable. Batch normalisation is an interface that enables every stage to learn more freely. Its purpose is to normalise the information from the previous levels and prevent that model from overfitting.[62]

Adam is used in our model as an optimizer and CrossEntropyloss for loss function.[63]

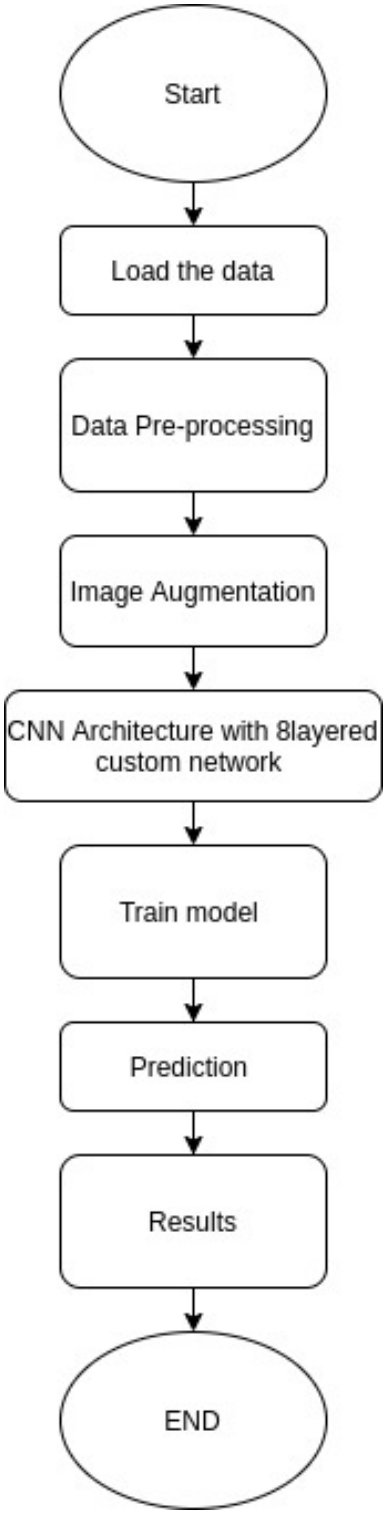

Figure 6.15: Custom Model Flow Diagram

Chapter 7

Dataset

DigitalGlobe's Open Data Program for Post-Hurricane Harvey was employed for this technique (In Texas). DigitalGlobe's WorldView-2 satellite, captured the photographs.

It consists of pre and post event Imagery over affected areas. The pre-events cover images from the year 2016 to the day Hurricane Harvey first occured. The post-event images have data of around a week after the Hurricane Harvey hit Texas.

The aim for using the dataset is to understand which region/s are likely to be damaged by floods. The good quality of images and high resolution makes it ideal for us.

Figure 7.1: Pre-Event Image

Figure 7.2: Post-Event

Link to the dataset : https://www.maxar.com/open-data/hurricane-harvey

Chapter 8

Plots for Accuracy and Loss with the number of epochs:

Accuracy vs Epoch Plot (Based on Hurricane Harvey Dataset):

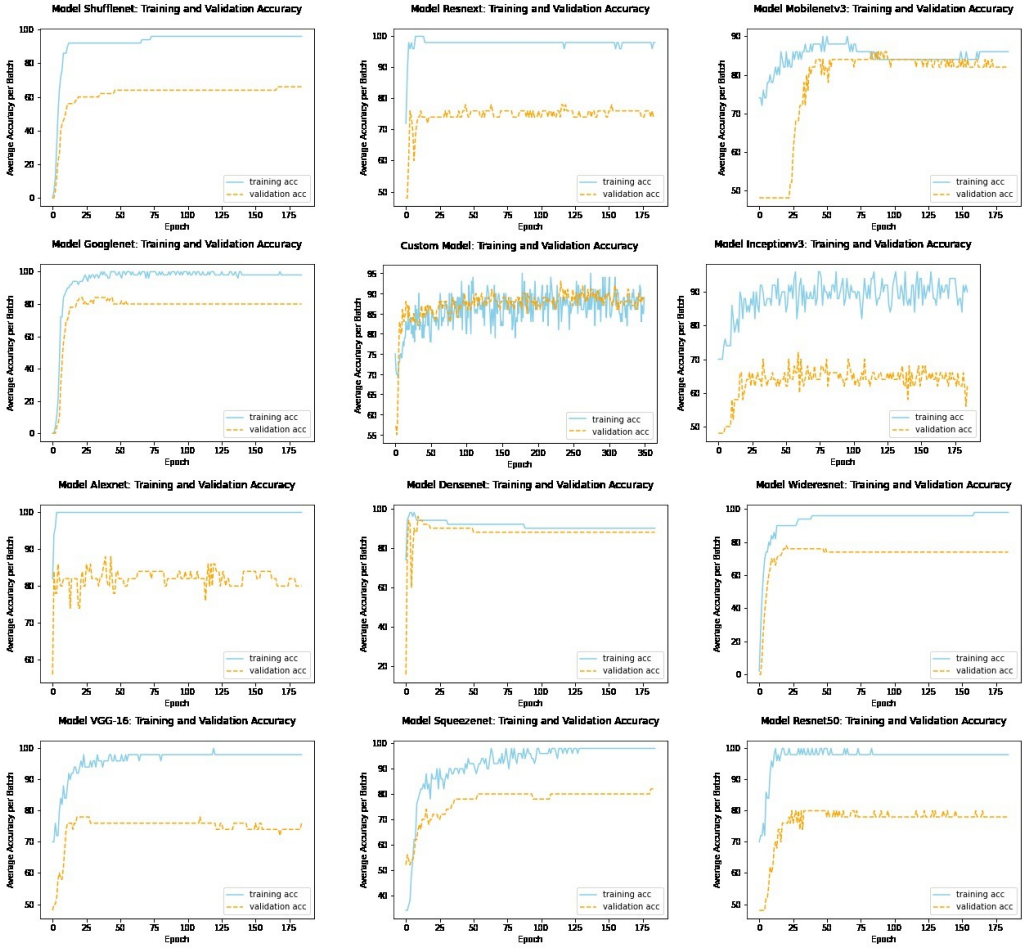

Loss vs Epoch Plot (Based on Hurricane Harvey Dataset):

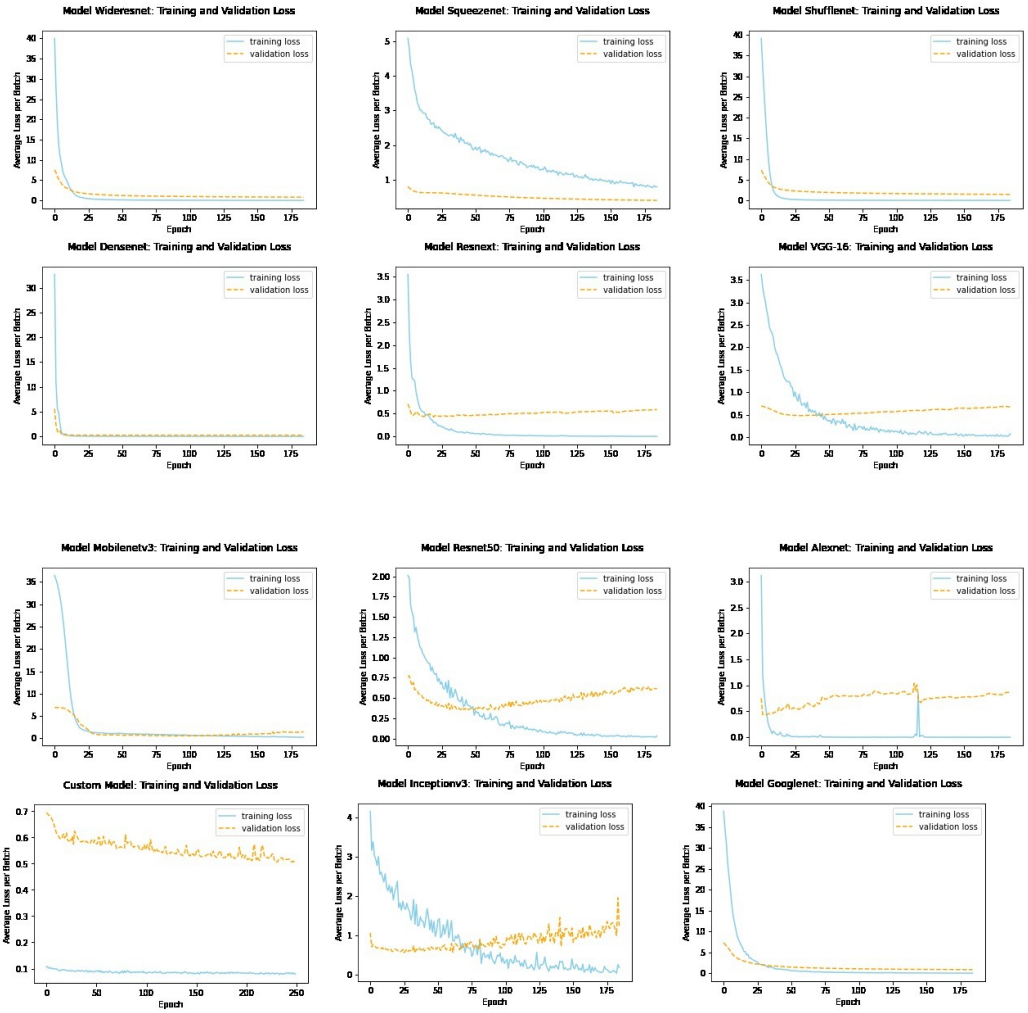

Accuracy vs Epoch Plot (Based on Custom Dataset):

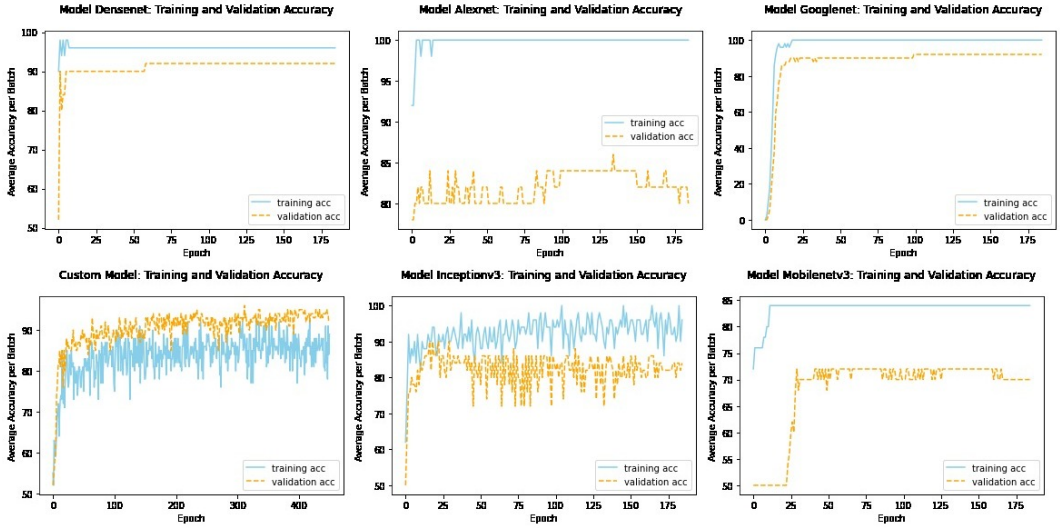

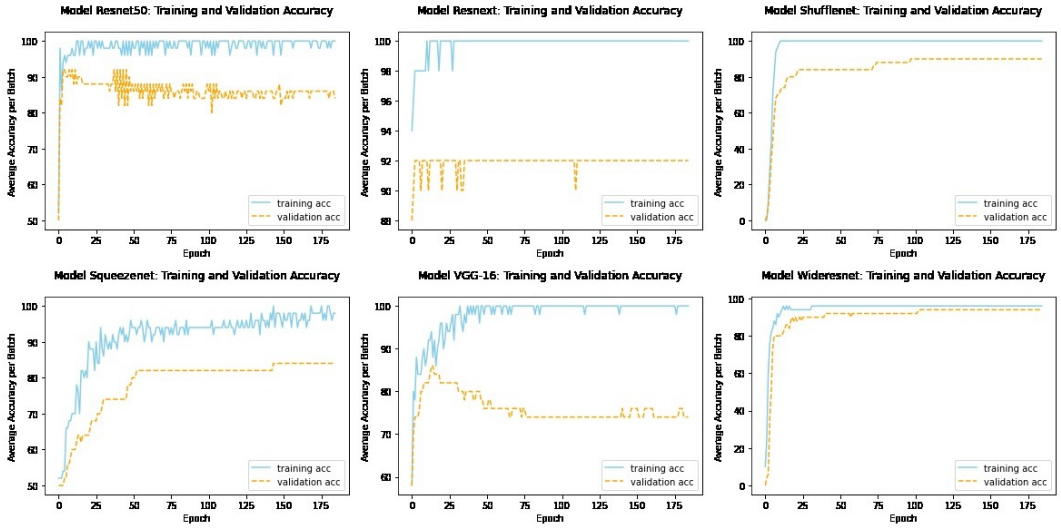

Loss vs Epoch Plot (Based on custom Dataset)

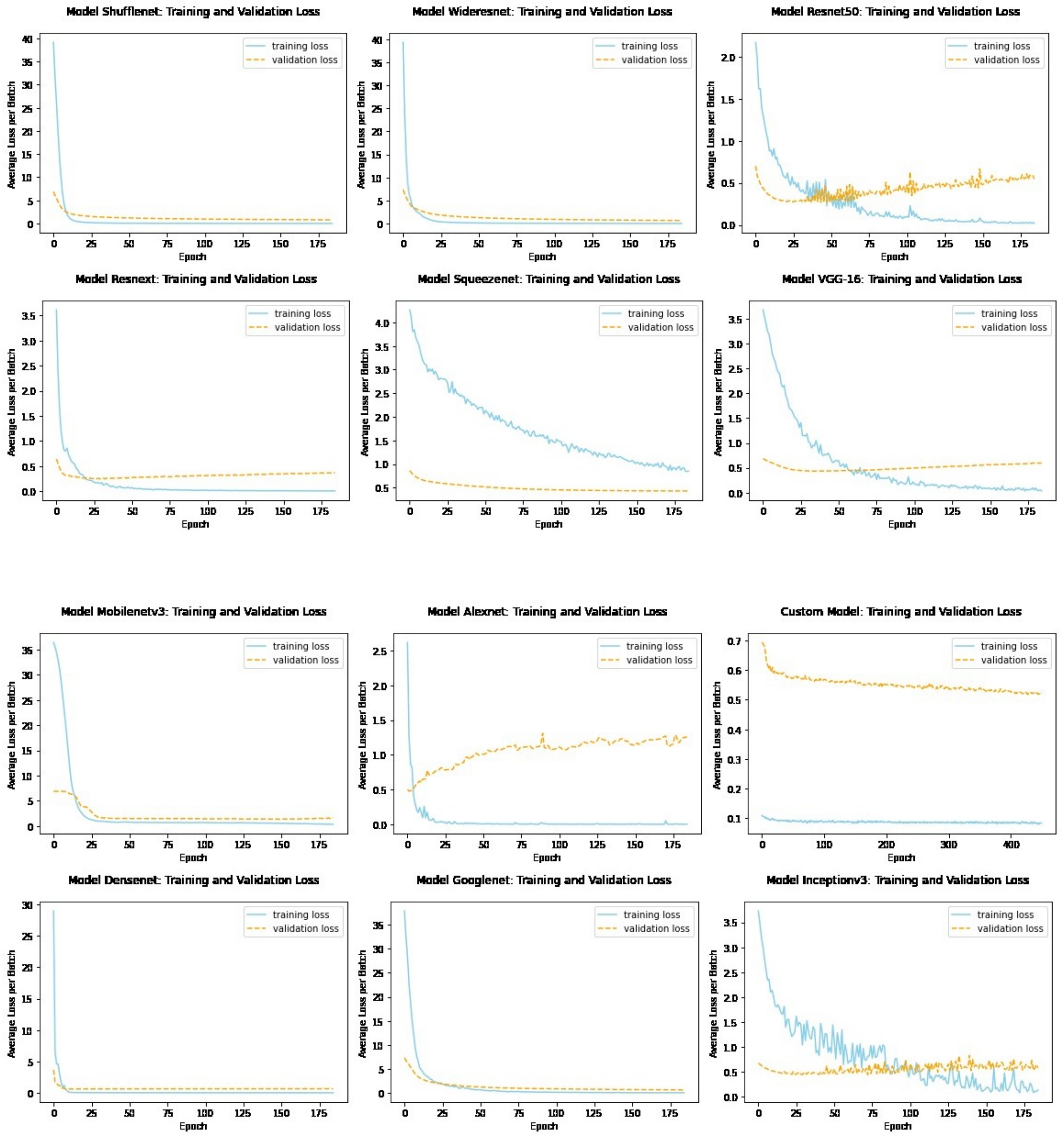

Loss comparison plot of all the 11 models

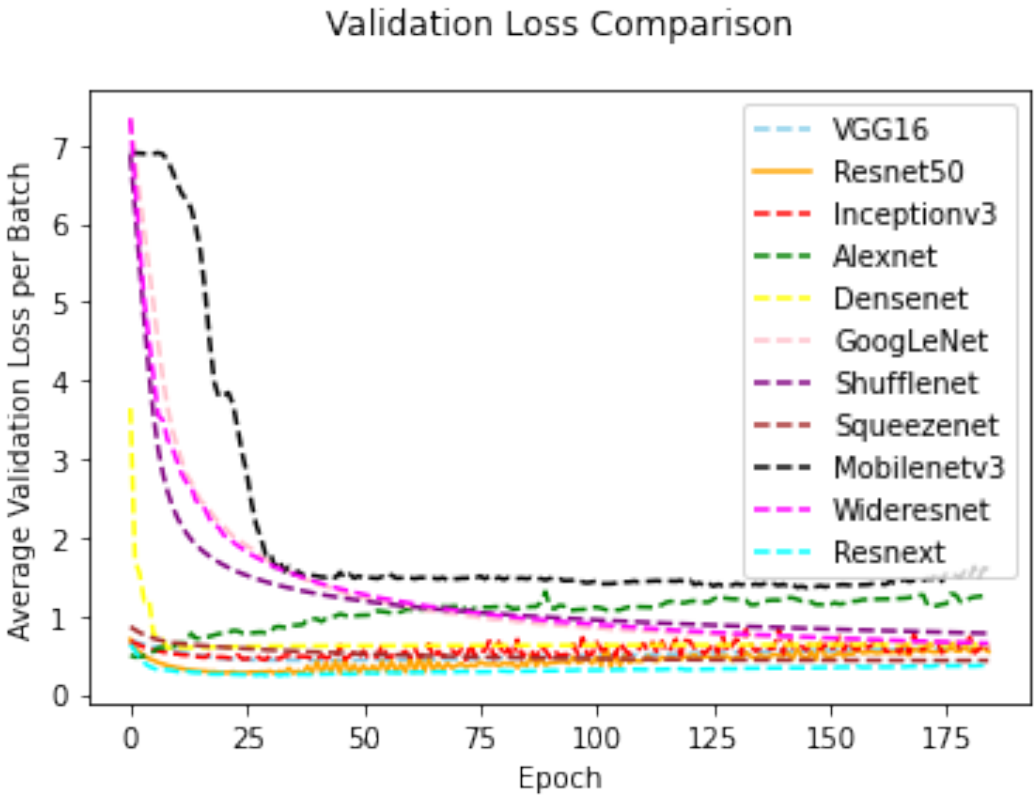

Figure 8.1: Loss comparison based on Custom Dataset

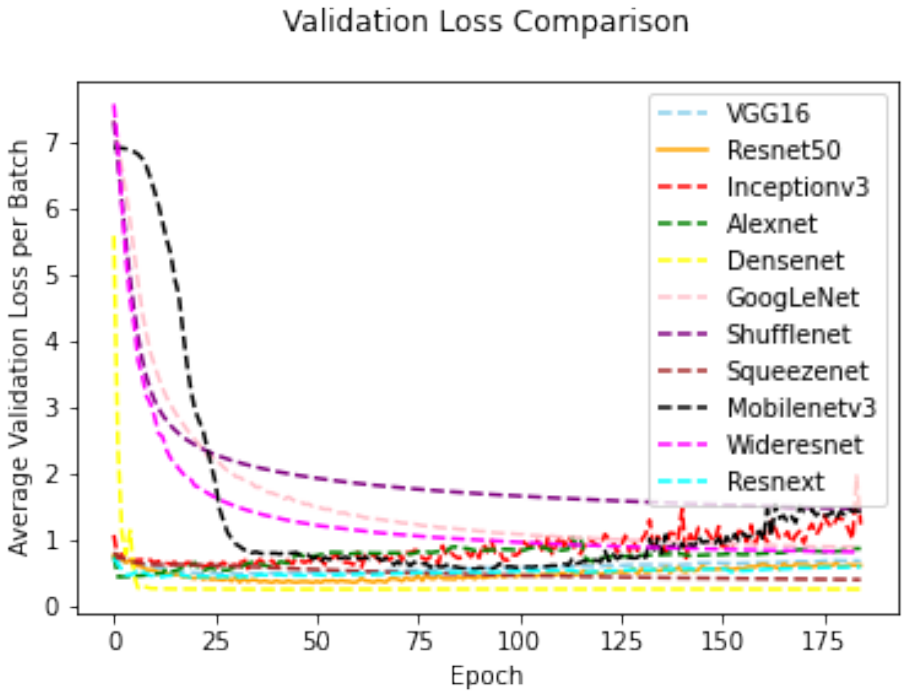

Figure 8.2: Loss comparison based on Hurricane Harvey Dataset

In both the graphs,validation loss is decreasing as the epochs increase. Using functions

such as Dropout, Adam optimizer and Cross Entropy loss has helped in minimizing the overfitting problem.

Chapter 9

Implementation

Dataset Source :DigitalGlobe's Open Data Program for Post-Hurricane Harvey is the first dataset chosen for this method (In Texas).

Experimented with 11 pre-trained models and compared with our custom model for 2 datasets. The 11 pre-trained models are: **VGG-16, Resnet50, Alexnet, Densenet, Inceptionv3, Squeezenet, Shufflenet, Googlenet, Wideresnet, Resnext,Mobilenet-v3**.

Programming Language:Python3

GPU Used: NVIDIA TESLA P100 GPU(Kaggle), NVIDIA Tesla K80 GPU(Google Colab).

Framework Used: Pytorch

Header Files used: Torch, Tensorflow, Torchvision, SKLearn,Numpy, PIL, Matplotlib, Seaborn.

Relu is the activation function employed. Dropout is a useful approach for regularisation because it prevents neuronal co-adaptation, which prevents overfitting. We utilised Adam Optimization and Cross Entropy loss to reduce overfitting. Adam Optimizer has a textbf0.0002 learning rate. Transfroms function were used for enhancing the quality of the images

transforms.Resize(), transforms.RandomHorizontalFlip(), transforms.ColorJitter(), transforms.ToTensor(), transforms.normalize().

Custom Model: It is used a custom model with eight layers. Input layer, Feature extraction, and Classification are the three phases of the network. The Feature Extraction phase includes three cnn architecture and three pooling layers. There is calculation with the help of the mathematical operation(dot operation) which takes in the input as well as the reception layers for the furthur analysis. All of the computation results in a

feature mapping being extracted from the image which is taken as input [61]
Avg-Pool, Max-pool are the two major pooling layers. Between the convolution layers are the two max-pool layers. Its goal is to aid in the reduction of overfitting. It takes the maximum of the area from the source that the kernel has covered. [61] The Avg-Pool Layer is like the Max-Pool Layer, only it takes the region's average. The Relu layer and the Batch Normalization layer are likewise fully coupled.
The activation function layer gives the model non-linearity, enabling it to learn complicated functional mappings between input data and target variable. Batch normalisation is a network layer that enables each layer to learn more freely from the others. It prevents this model from overfitting by normalising the output of the previous layers. [62]
The HyperParameters like Batch Size and Learning Rate are also adjusted. For the optimization, we choose Adam Optimizer as the model optimizer which has a learning rate of 0.0003 and CrossEntropyLoss as the function loss.

Following are the training, validation, testing images after applying various preprocessing, data optimizing techniques.

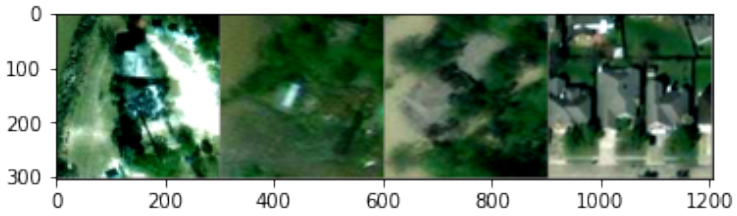

Figure 9.1: Training images

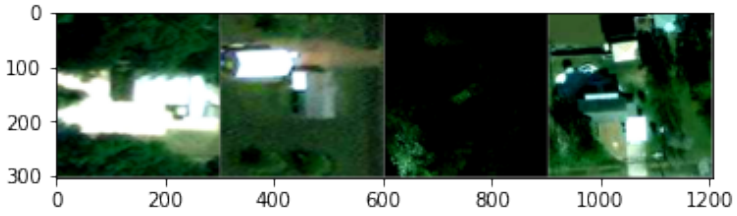

Figure 9.2: Validation Images

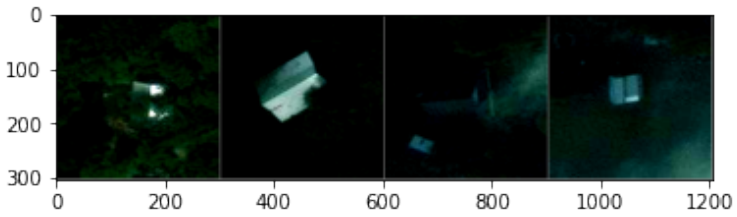

Figure 9.3: Testing Diagram

Chapter 10

Performance Metrics

Both the table shows the the performance metrics based on both the datasets. The first shows for Hurricane Harvey dataset, the second for custom Dataset. For the Hurricane Harvey Dataset, Resnet 50 is showing the highest accuracy of 93.56 %. For the Custom Dataset, GoogleNet shows a accuracy of 90.65 %.

For both the datasets, the custom model has maintained above 90% accuracy. In the case of Hurricane Harvey Dataset, it has an accuracy of 91.44% and for the Custom Dataset it has a accuracy of 90.17%.

10.1 Performance Metrics

10.1.1 (A) Hurricane Harvey Dataset

Model Name	ACCURACY	PRECISION	RECALL	F1-SCORE
Vgg-16	0.8977	0.9183	0.9649	0.9410
Resnet-50	0.9356	0.9530	0.9739	0.9634
Inception_v3	0.8938	0.9593	0.9241	0.9414
Alexnet	0.8963	0.9058	0.9759	0.9395
Densenet	0.9350	0.9500	0.9762	0.9629
GoogleNet	0.9103	0.9402	0.9581	0.9491
Shufflenet	0.8796	0.9127	0.9491	0.9305
Squeezenet	0.9108	0.9296	0.9687	0.9488
Wideresnet	0.8735	0.8836	0.9712	0.9253
Resnext	0.8921	0.9304	0.9473	0.9388
Mobilenet-v3	0.7407	0.7548	0.9420	0.8380
Custom Model	0.9144	0.9293	0.9733	0.9508

10.1.2 (B) Custom Dataset

Model Name	ACCURACY	PRECISION	RECALL	F1-SCORE
Vgg-16	0.8708	0.8812	0.9708	0.9238
Resnet-50	0.8909	0.9058	0.9695	0.9366
Inception_v3	0.7947	0.7842	0.9811	0.8717
Alexnet	0.8688	0.8718	0.9783	0.9220
Densenet	0.8940	0.8913	0.9884	0.9373
GoogleNet	0.9065	0.9158	0.9775	0.9456
Shufflenet	0.8250	0.8993	0.8881	0.8936
Squeezenet	0.8914	0.8982	0.9779	0.9363
Wideresnet	0.8029	0.7873	0.9871	0.8760
Resnext	0.8877	0.8835	0.9890	0.9333
Mobilenet-v3	0.7479	0.7532	0.9534	0.8416
Custom Model	0.9017	0.9042	0.9840	0.9424

Chapter 11

Inferences from Dataset

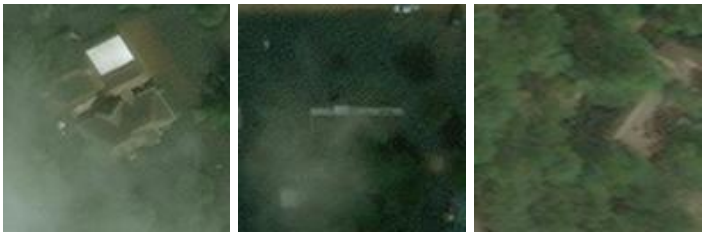

Figure 11.1: Blur Images

The angle in which the images are seen, some images may be taken from a different angle thereby becoming difficult to identify the images . Apart from this, shadows and blurry images may result in lack of clarity. This accounted for approximately 6

Depending on whether the images was taken when during or night along with fog or dust makes a big difference as illumination may lead to the same object to look different depending on the lighting conditions.This accounted for approximately 5-6

At times the damaged areas may have blended with the surrounding area thereby making it more complicated to detect. Object localization problem might occur where the location of the damaged building might not be properly located, thereby reducing the accuracy.

At times object localization might have bounded boxes on the wrong object, so the need of loss criterion is a must.

For reducing the effect of overfitting and for improving the accuracy, the loss criterion function was used, which helped in minimizing the object localization errors.

Adam Optimizer was chosen with a learning rate 0.0002, improved the performance. It is efficient in the sense, that it requires very less memory/ RAM space, has an efficient performance even with large datasets and it has better distribution of weights.

All the models are using many layers and with activation function, it can lead to the vanishing gradient problem, where derivative becomes very small thereby accuracy is lowered.For resolving this, applying the Cross entropy function helped inimproving the performance.

Chapter 12

Conclusion

In this paper, a thorough literature review and implementation of - 'Damage Detection of buildings and roads using Satellite Images' has been carried out. Many existing research works show errors while detection due to an overfitting problem, thereby misclassifying damaged structures as not damaged. This paper tries to minimize the overfitting issues by combining two different datasets with two different orientations obtaining the accuracy of 91.44 and 90.17 for the hurricane Harvey Dataset and Custom Dataset repectively for the Custom Model. Furthermore, one of the most significant difficulties of object detection using satellite imagery is that an object viewed from different angles may look completely different and this is the future scope that needs to be considered.

We have done a comparison among the various models,and from the test accuracies, we see that for both the datasets, the custom model and Googlenet are a good choice as the test accuracies for both these models in both the datasets is above 90%.

We will further be conducting more research on these proposed models and improving accuracy of damage detection.

Chapter 13

Timeline

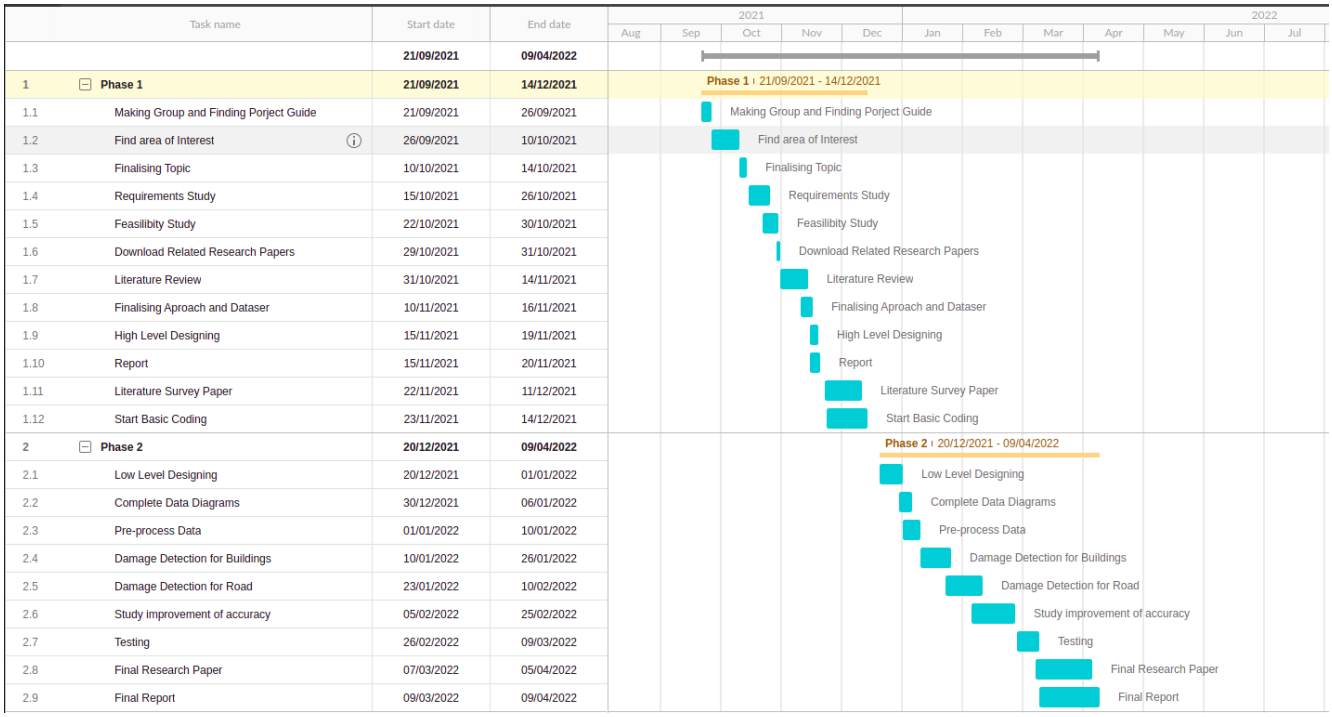

	Task name	Start date	End date
		21/09/2021	**09/04/2022**
1	**Phase 1**	**21/09/2021**	**14/12/2021**
1.1	Making Group and Finding Porject Guide	21/09/2021	26/09/2021
1.2	Find area of Interest	26/09/2021	10/10/2021
1.3	Finalising Topic	10/10/2021	14/10/2021
1.4	Requirements Study	15/10/2021	26/10/2021
1.5	Feasilibity Study	22/10/2021	30/10/2021
1.6	Download Related Research Papers	29/10/2021	31/10/2021
1.7	Literature Review	31/10/2021	14/11/2021
1.8	Finalising Aproach and Dataser	10/11/2021	16/11/2021
1.9	High Level Designing	15/11/2021	19/11/2021
1.10	Report	15/11/2021	20/11/2021
1.11	Literature Survey Paper	22/11/2021	11/12/2021
1.12	Start Basic Coding	23/11/2021	14/12/2021
2	**Phase 2**	**20/12/2021**	**09/04/2022**
2.1	Low Level Designing	20/12/2021	01/01/2022
2.2	Complete Data Diagrams	30/12/2021	06/01/2022
2.3	Pre-process Data	01/01/2022	10/01/2022
2.4	Damage Detection for Buildings	10/01/2022	26/01/2022
2.5	Damage Detection for Road	23/01/2022	10/02/2022
2.6	Study improvement of accuracy	05/02/2022	25/02/2022
2.7	Testing	26/02/2022	09/03/2022
2.8	Final Research Paper	07/03/2022	05/04/2022
2.9	Final Report	09/03/2022	09/04/2022

Bibliography

[1] Cao, Q. & Choe, Y., 2021. Building damage annotation on post-hurricane satellite imagery based on convolutional neural networks.

[2] Kaur, S., Gupta, S., Singh, S., Koundal, D. & Zaguia, A., 2021. Convolutional Neural Network based Hurricane Damage Detection using Satellite Images. [online] Available at: ¡https://assets.researchsquare.com/files/rs-934531/v1/61a71f08-c163-442b-a62e-1af4cdc8708d.pdf?c=1632928070¿.

[3] Cao, Q. & Choe, Y., 2021. Post-Hurricane Damage Assessment Using Satellite Imagery and Geolocation Features. [online] Arxiv.org. Available at: ¡https://arxiv.org/pdf/2012.08624.pdf¿ [Accessed 20 November 2021].

[4] Shinozuka, M., Ghanem, R., Houshmand, B., & Mansouri, B. (2000). Damage Detection in Urban Areas by SAR Imagery. In Journal of Engineering Mechanics (Vol. 126, Issue 7, pp. 769–777). American Society of Civil Engineers (ASCE). https://doi.org/10.1061/(asce)0733-9399(2000)126:7(769)

[5] G. Andre, L. Chiroiu, C. Mering, & F. Chopin, "Building destruction and damage assessment after earthquake using high resolution optical sensors. The case of the Gujarat earthquake of January 26, 2001," IGARSS 2003. 2003 IEEE International Geoscience and Remote Sensing Symposium. Proceedings (IEEE Cat. No.03CH37477). IEEE [Online]. Available: http://dx.doi.org/10.1109/IGARSS.2003.1294454

[6] M. Chini, C. Bignami, S. Stramondo, W. J. Emery, & N. Pierdicca, "Quickbird Panchromatic Images for Mapping Damage at Building Scale Caused by the 2003 Bam Earthquake," IGARSS 2008 - 2008 IEEE International Geoscience and Remote Sensing Symposium. IEEE, 2008 [Online]. Available: http://dx.doi.org/10.1109/IGARSS.2008.4779173

[7] Yamazaki, F.. (2005). Damage detection based on object-based segmentation and classification from high-resolution satellite images for the 2003 boumerdes, algeria earthquake.

[8] Yamazaki, F. & Kouchi, Ken & Kohiyama, Masayuki & Muraoka, Nanae & Matsuoka, Masashi. (2004). Earthquake damage detection using high-resolution satellite images. 4. 2280 - 2283 vol.4. 10.1109/IGARSS.2004.1369739.

[9] Yamazaki, F. & Yano, Y. & Matsuoka, Masashi. (2005). Damage detection in earthquake disasters using high-resolution satellite images.

[10] S. Stramondo, C. Bignami, N. Pierdicca & M. Chini, "SAR and optical remote sensing for urban damage detection and mapping: case studies," 2007 Urban Remote Sensing Joint Event, 2007, pp. 1-6, doi: 10.1109/URS.2007.371866.

[11] Turker, Mustafa & Sumer, Emre. (2008). Building-based damage detection due to earthquake using the watershed segmentation of the post-event aerial images. International Journal of Remote Sensing. 29. 3073-3089. 10.1080/01431160701442096.

[12] Geshi, S., DISASTER DAMAGE DETECTION AND ITS RECOVERY SUPPORT SYSTEM OF ROAD AND RAILROAD USING SATELLITE IMAGES.

[13] Xianglong, Liu et al. "Large-scale highway disaster assessment of earthquake using GIS and remote sensing." 2010 Second IITA International Conference on Geoscience and Remote Sensing 2 (2010): 174-178.

[14] C. D. Parape and M. Tamura, "Identifying damaged buildings from high-resolution satellite imagery in hazardous areas using morphological operators," 2011 IEEE International Geoscience and Remote Sensing Symposium, 2011, pp. 1898-1901, doi: 10.1109/IGARSS.2011.6049495.

[15] S. Koshimura, S. Kayaba and H. Gokon, "Object-based image analysis of post-tsunami high-resolution satellite images for mapping the impact of tsunami disaster," 2011 IEEE International Geoscience and Remote Sensing Symposium, 2011, pp. 1993-1996, doi: 10.1109/IGARSS.2011.6049519.

[16] X. Tong et al., "Building-damage detection using pre- and post-seismic high-resolution satellite stereo imagery: A case study of the May 2008 Wenchuan earthquake," ISPRS Journal of Photogrammetry and Remote

Sensing, vol. 68. Elsevier BV, pp. 13–27, Mar-2012 [Online]. Available: http://dx.doi.org/10.1016/j.isprsjprs.2011.12.004

[17] Uprety, Pralhad & Yamazaki, F.. (2012). Use of high-resolution SAR intensity images for damage detection from the 2010 Haiti earthquake. International Geoscience and Remote Sensing Symposium (IGARSS). 6829-6832. 10.1109/IGARSS.2012.6352595.

[18] Dong, Laigen & Shan, Jie. (2013). A comprehensive review of earthquake-induced building damage detection with remote sensing techniques. ISPRS Journal of Photogrammetry and Remote Sensing. 84. 85–99. 10.1016/j.isprsjprs.2013.06.011.

[19] H. Ma, N. Lu, L. Ge, Q. Li, X. You and X. Li, "Automatic road damage detection using high-resolution satellite images and road maps," 2013 IEEE International Geoscience and Remote Sensing Symposium - IGARSS, 2013, pp. 3718-3721, doi: 10.1109/IGARSS.2013.6723638.

[20] M. P. Herfeh, A. Shahbahrami and F. P. Miandehi, "Detecting earthquake damage levels using adaptive boosting," 2013 8th Iranian Conference on Machine Vision and Image Processing (MVIP), 2013, pp. 251-256, doi: 10.1109/IranianMVIP.2013.6779989.

[21] B. Adriano, H. Gokon, E. Mas, S. Koshimura, W. Liu and M. Matsuoka, "Extraction of damaged areas due to the 2013 Haiyan Typhoon using ASTER data," 2014 IEEE Geoscience and Remote Sensing Symposium, 2014, pp. 2154-2157, doi: 10.1109/IGARSS.2014.6946893.

[22] X. Zhang, Y. Chen, M. Jia, L. Tong, Y. Lu and Y. Cao, "The study of road damage detection based on high-resolution SAR image," 2013 IEEE International Geoscience and Remote Sensing Symposium - IGARSS, 2013, pp. 2633-2636, doi: 10.1109/IGARSS.2013.6723363.

[23] Hassanzadeh, Reza & Nedovic-Budic, Zorica. (2014). Assessment of the Contribution of Crowd Sourced Data to Post-Earthquake Building Damage Detection. International Journal of Information Systems for Crisis Response and Management. 6. 1-37. 10.4018/ijiscram.2014010101.

[24] J. Wang et al., "A knowledge-based method for road damage detection using high-resolution remote sensing image," 2015 IEEE International Geo-

science and Remote Sensing Symposium (IGARSS), 2015, pp. 3564-3567, doi: 10.1109/IGARSS.2015.7326591.

[25] M. O. Sghaier and R. Lepage, "Road damage detection from VHR remote sensing images based on multiscale texture analysis and dempster shafer theory," 2015 IEEE International Geoscience and Remote Sensing Symposium (IGARSS), 2015, pp. 4224-4227, doi: 10.1109/IGARSS.2015.7326758.

[26] Janalipour, Milad & Mohammadzadeh, Ali. (2015). ¬Building Damage Detection Using Object Based Image Analysis and ANFIS from High Resolution Image (Case Study: BAM earthquake, Iran). IEEE Journal of Selected Topics in Applied Earth Observations and Remote Sensing. PP. 1 - 9. 10.1109/JSTARS.2015.2458582.

[27] L. Gueguen and R. Hamid, "Large-scale damage detection using satellite imagery," 2015 IEEE Conference on Computer Vision and Pattern Recognition (CVPR), 2015, pp. 1321-1328, doi: 10.1109/CVPR.2015.7298737.

[28] D. Dubois and R. Lepage, "Ensemble classifiers for building damage detection," 2015 IEEE International Geoscience and Remote Sensing Symposium (IGARSS), 2015, pp. 2715-2718, doi: 10.1109/IGARSS.2015.7326374.

[29] Chu, Edward & Wu, Chung-Chih. (2015). An image-based seismic damage assessment system. Multimedia Tools and Applications. 75. 10.1007/s11042-015-2602-9.

[30] A. Menderes, A. Erener, and G. Sarp, "Automatic Detection of Damaged Buildings after Earthquake Hazard by Using Remote Sensing and Information Technologies," Procedia Earth and Planetary Science, vol. 15. Elsevier BV, pp. 257–262, 2015 [Online]. Available: http://dx.doi.org/10.1016/j.proeps.2015.08.063

[31] F. Kahraman, M. Imamoglu and H. F. Ates, "Disaster damage assessment for buildings using self-similarity descriptor," 2015 IEEE International Geoscience and Remote Sensing Symposium (IGARSS), 2015, pp. 2711-2714, doi: 10.1109/IGARSS.2015.7326373.

[32] Tu, Jihui & Sui, Haigang & Feng, Wenqing & Song, Zhina. (2016). AUTOMATIC BUILDING DAMAGE DETECTION METHOD USING HIGH-RESOLUTION REMOTE SENSING IMAGES AND 3D GIS MODEL. ISPRS Annals of Photogrammetry, Remote Sensing and Spatial Information Sciences. III-8. 43-50. 10.5194/isprsannals-III-8-43-2016.

[33] Yamazaki, F. & Liu, Wen & Bahri, Rendy & Sasagawa, Tadashi. (2016). Damage extraction of buildings in the 2015 Gorkha, Nepal earthquake from high-resolution SAR data. 98772K. 10.1117/12.2223306.

[34] Gong, Lixia & Wang, Chao & Wu, Fan & Zhang, Jingfa & Zhang, Hong & Li, Qiang. (2016). Earthquake-Induced Building Damage Detection with Post-Event Sub-Meter VHR TerraSAR-X Staring Spotlight Imagery. Remote Sensing. 8. 887. 10.3390/rs8110887.

[35] F. Kahraman, M. Imamoglu and H. F. Ates, "Battle Damage Assessment based on self-similarity and contextual modeling of buildings in dense urban areas," 2016 IEEE International Geoscience and Remote Sensing Symposium (IGARSS), 2016, pp. 5161-5164, doi: 10.1109/IGARSS.2016.7730345.

[36] D. M. Hordiiuk and V. V. Hnatushenko, "Neural network and local laplace filter methods applied to very high resolution remote sensing imagery in urban damage detection," 2017 IEEE International Young Scientists Forum on Applied Physics and Engineering (YSF), 2017, pp. 363-366, doi: 10.1109/YSF.2017.8126648.

[37] Cha, Young-Jin & Choi, Wooram & Buyukozturk, Oral. (2017). Deep Learning-Based Crack Damage Detection Using Convolutional Neural Networks. Computer-Aided Civil and Infrastructure Engineering. 32. 361-378. 10.1111/mice.12263.

[38] A. Fujita, K. Sakurada, T. Imaizumi, R. Ito, S. Hikosaka and R. Nakamura, "Damage detection from aerial images via convolutional neural networks," 2017 Fifteenth IAPR International Conference on Machine Vision Applications (MVA), 2017, pp. 5-8, doi: 10.23919/MVA.2017.7986759.

[39] Sharma, Ram C. & Tateishi, Ryutaro & Hara, Keitarou & Hoan, Nguyen & Gharechelou, Saeid & Nguyen Viet, Luong. (2017). Earthquake Damage Visualization (EDV) Technique for the Rapid Detection of Earthquake-Induced Damages Using SAR Data. Sensors. 17. 235. 10.3390/s17020235.

[40] Zhou, Zixiang & Gong, Jie. (2018). Automated residential building detection from airborne LiDAR data with deep neural networks. Advanced Engineering Informatics. 36. 229-241. 10.1016/j.aei.2018.04.002.

[41] Doshi, Jigar & Basu, Saikat & Pang, Guan. (2018). From Satellite Imagery to Disaster Insights.

[42] Maeda, Hiroya & Sekimoto, Yoshihide & Seto, Toshikazu & Kashiyama, Takehiro & Omata, Hiroshi. (2018). Road Damage Detection and Classification Using Deep Neural Networks with Smartphone Images: Road damage detection and classification. Computer-Aided Civil and Infrastructure Engineering. 33. 10.1111/mice.12387.

[43] Li, Qiang & Gong, Lixia & Zhang, Jingfa. (2018). Earthquake-induced building detection based on object-level texture feature change detection of multitemporal sar images. Boletim de Ciências Geodésicas. 24. 442-458. 10.1590/s1982-21702018000400028.

[44] Kashif Ahmad, Konstantin Pogorelov, Michael Riegler, Olga Ostroukhova, Pål Halvorsen, Nicola Conci, Rozenn Dahyot, Automatic detection of passable roads after floods in remote sensed and social media data, Signal Processing: Image Communication, ISSN 0923-5965, https://doi.org/10.1016/j.image.2019.02.002.

[45] Xu, Joseph & Lu, Wenhan & Li, Zebo & Khaitan, Pranav & Zaytseva, Valeriya. (2019). Building Damage Detection in Satellite Imagery Using Convolutional Neural Networks.

[46] Khodaverdi, Niloofar & Rastiveis, Heidar & Jouybari, Arash. (2019). Combination of Post-Earthquake LiDAR Data and Satellite Imagery for Buildings Damage Detection. 3. 12-20. 10.22059/eoge.2019.278307.1046.

[47] Hoppe, Edward & Novali, Fabrizio & Rucci, Alessio & Fumagalli, Alfio & Del Conte, Sara & Falorni, Giacomo & Toro, Nora. (2019). Deformation Monitoring of Posttensioned Bridges Using High-Resolution Satellite Remote Sensing. Journal of Bridge Engineering. 24. 04019115. 10.1061/(ASCE)BE.1943-5592.0001479.

[48] Nex, Francesco & Duarte, Diogo & Giulio Tonolo, Fabio & Kerle, Norman. (2019). Structural Building Damage Detection with Deep Learning: Assessment of a State-of-the-Art CNN in Operational Conditions. Remote Sensing. 11. 2765. 10.3390/rs11232765.

[49] Ghaffarian, Saman & Kerle, Norman. (2019). TOWARDS POST-DISASTER DEBRIS IDENTIFICATION FOR PRECISE DAMAGE AND RECOVERY ASSESSMENTS FROM UAV AND SATELLITE IMAGES. ISPRS - International Archives of the Photogrammetry, Remote Sensing and Spatial Information Sciences. XLII-2/W13. 297-302. 10.5194/isprs-archives-XLII-2-W13-297-2019.

[50] Meilano, Irwan et al. “Analysis of Damage to Buildings affected by the Tsunami in the Palu Coastal Area Using Deep Learning.” 2020 IEEE Asia-Pacific Conference on Geoscience, Electronics and Remote Sensing Technology (AGERS) (2020): 95-97.

[51] F. Zhao, J. Bao and D. Ming, ”Battle Damage Assessment for Building based on Multi-feature,” 2020 IEEE 5th Information Technology and Mechatronics Engineering Conference (ITOEC), 2020, pp. 57-60, doi: 10.1109/ITOEC49072.2020.9141701.

[52] X. Jiang, Y. He, G. Li, Y. Liu and X. Zhang, ”Building Damage Detection via Superpixel-Based Belief Fusion of Space-Borne SAR and Optical Images,” in IEEE Sensors Journal, vol. 20, no. 4, pp. 2008-2022, 15 Feb.15, 2020, doi: 10.1109/JSEN.2019.2948582.

[53] S. -E. Park and S. -G. Lee, ”Change Detection of Urban Areas Affected by Earthquake Using Kompsat-5 Data,” IGARSS 2020 - 2020 IEEE International Geoscience and Remote Sensing Symposium, 2020, pp. 3568-3570, doi: 10.1109/IGARSS39084.2020.9323162.

[54] Gupta, R., Hosfelt, R., Sajeev, S., Patel, N., Goodman, B., Doshi, J., Heim, E., Choset, H. and Gaston, M., 2021. xBD: A Dataset for Assessing Building Damage from Satellite Imagery. [online] arXiv.org. Available at: ¡https://arxiv.org/abs/1911.09296¿.

[55] Saganeiti, L., Amato, F., Nolè, G., Vona, M. and Murgante, B., 2021. Early estimation of ground displacements and building damage after seismic events using SAR and LiDAR data: The case of the Amatrice earthquake in central Italy, on 24th August 2016.

[56] Gupta, Rohit & Shah, Mubarak. (2021). RescueNet: Joint Building Segmentation and Damage Assessment from Satellite Imagery. 4405-4411. 10.1109/ICPR48806.2021.9412295.

[57] T. Miyamoto & Y. Yamamoto, ”Using Multimodal Learning Model for Earthquake Damage Detection Based on Optical Satellite Imagery and Structural Attributes,” IGARSS 2020 - 2020 IEEE International Geoscience and Remote Sensing Symposium, 2020, pp. 6623-6626, doi: 10.1109/IGARSS39084.2020.9324464.

[58] Cao, Quoc Dung & Choe, Youngjun. (2020). Building damage annotation on post-hurricane satellite imagery based on convolutional neural networks. Natural Hazards. 103. 10.1007/s11069-020-04133-2.

[59] W. Zhang, L. Shen & W. Qiao, "Building Damage Detection in Vhr Satellite Images Via Multi-Scale Scene Change Detection," 2021 IEEE International Geoscience and Remote Sensing Symposium IGARSS, 2021, pp. 8570-8573, doi: 10.1109/IGARSS47720.2021.9554922.

[60] M. Zhang & Z. Chen, "Deep Metric Learning for Damage Detection Using Bitemporal Satellite Images," 2021 IEEE International Geoscience and Remote Sensing Symposium IGARSS, 2021, pp. 562-565, doi: 10.1109/IGARSS47720.2021.9553775.

[61] Convolutional Neural Networks in Python. (n.d.). DataCamp Community. https://www.datacamp.com/community/tutorials/convolutional-neural-networks-python

[62] Dwivedi, R. (n.d.). Everything You Should Know About Dropouts And BatchNormalization In CNN. Analytics India Magazine. https://analyticsindiamag.com/everything-you-should-know-about-dropouts-and-batchnormalization-in-cnn/

[63] Koppert-Anisimova, I. (n.d.). Cross-Entropy Loss in ML - unpackAI. Medium. https://medium.com/unpackai/cross-entropy-loss-in-ml-d9f22fc11fe0

[64] Muneeb ul Hassan . VGG16 – Convolutional Network for Classification and Detection https://neurohive.io/en/popular-networks/vgg16/

[65] Kaushik, A. (n.d.). Understanding ResNet50 architecture. OpenGenus IQ: Computing Expertise & Legacy. https://iq.opengenus.org/resnet50-architecture/

[66] Karen Simonyan & Andrew Zisserman, "VERY DEEP CONVOLUTIONAL NETWORKS FOR LARGE-SCALE IMAGE RECOGNITION", https://arxiv.org/pdf/1409.1556.pdf

[67] Kaiming He, Xiangyu Zhang, Shaoqing Ren, Jian Sun," Deep Residual Learning for Image Recognition", https://arxiv.org/abs/1512.03385

[68] Jonathon Shlens, Sergey Ioffe, Vincent Vanhoucke, Christian Szegedy, Zbigniew Wojna,"Rethinking the Inception Architecture for Computer Vision", https://arxiv.org/pdf/1512.00567.pdf

[69] Gao Huang, Zhuang Liu, Laurens van der Maaten, Kilian Q. Weinberger, "Densely Connected Convolutional Networks",https://arxiv.org/abs/1608.06993

[70] Md Zahangir Alom1, Tarek M. Taha1, Chris Yakopcic, Stefan Westberg, Paheding Sidike, Mst Shamima Nasrin1,Brian C Van Essen3, Abdul A S. Awwal , and Vijayan K. Asari1, "The History Began from AlexNet: A Comprehensive Survey on Deep Learning Approaches" ,https://arxiv.org/pdf/1803.01164.pdf

[71] Christian Szegedy, Wei Liu, Yangqing Jia, Pierre Sermanet, Scott Reed,Dragomir Anguelov, Dumitru Erhan, Vincent Vanhoucke, Andrew Rabinovich, "Going deeper with convolutions", https://arxiv.org/pdf/1409.4842.pdf

[72] Saining Xie, Ross Girshick, Piotr Dollár, Zhuowen Tu, Kaiming He, "Aggregated Residual Transformations for Deep Neural Networks", https://arxiv.org/abs/1611.05431

[73] Sergey Zagoruyko, Nikos Komodakis, "Wide Residual Networks", https://arxiv.org/abs/1605.07146

[74] Xiangyu Zhang, Xinyu Zhou, Mengxiao Lin, Jian Sun ,"ShuffleNet: An Extremely Efficient Convolutional Neural Network for Mobile Devices" https://arxiv.org/abs/1707.01083

[75] Forrest N. Iandola, Song Han, Matthew W. Moskewicz, Khalid Ashraf, William J. Dally, Kurt Keutzer,"SqueezeNet: AlexNet-level accuracy with 50x fewer parameters and ¡0.5MB model size", https://arxiv.org/abs/1602.07360

[76] Andrew G. Howard, Menglong Zhu, Bo Chen, Dmitry Kalenichenko, Weijun Wang, Tobias Weyand, Marco Andreetto, Hartwig Adam, "MobileNets: Efficient Convolutional Neural Networks for Mobile Vision Applications ", https://arxiv.org/abs/1704.04861